THE SLIDING WEAR OF POLYMERS AGAINST STEEL

by

C.G. CLARKE

A thesis submitted to the Faculty of Engineering at the University of Cape Town in fulfilment of the degree of Master of Science

Department of Materials Engineering
University of Cape Town

DECEMBER 1988

ACKNOWLEDGEMENTS

I would like to thank all the people who assisted me in this project and contributed to its completion. In particular I would like to thank

Professor Colin Allen, my supervisor, for his interest, advice and support through difficult times.

Mr Nicholas Dreze, Mr Glen Newins and Mr Martin Batho for their assistance in the assembly and maintenance of experimental apparatus.

Mr Dave Dean for his electronics expertise.

Mrs Helgard Bohm, Mrs Sue Betz and Mrs Penny Park-Ross for their technical assistance and for their help in the preparation of this manuscript.

Mr Bernard Greeves and Mr James Peterson for their photographic expertise.

Mrs Anne Ball and Mrs Jane Geldenhuys for the typing of this manuscript.

The work described in this thesis was performed under a collaborative agreement between the Chamber of Mines of South Africa and the University of Cape Town and formed part of the research programme of the Research Organisation of the Chamber of Mines.

ABSTRACT

A laboratory wear testing facility has been developed to generate wear rate data for polymeric materials sliding at constant velocity against a hardened stainless steel base. The polymers investigated were ultra high molecular weight polyethylene (UHMWPE), ultra high molecular weight polyethylene with a friction reducing additive (UHMWPE/FILL), polyoxymethylene (POM), poly(ethylene terephthalate) (PETP), molybdenum disulphide filled polyamide 6 (PA6/MoS_2) and graphite filled poly(amide-imide) (P(A-I)/GR). Testing was carried out as a function of sliding velocity between 0.13 to 2.27 ms^{-1}, loads of 1, 3 and 5 MPa and counterface roughnesses which varied from 1 micrometre to 0.25 micrometres.

An increase in the counterface roughness resulted in a variable increase in the wear rate of the individual polymers except for the filled UHMWPE. These changes in the wear rate have been explained in terms of the mechanism of material removal. A progressive increase in sliding velocity has been shown to result in an initial increase in the wear rate followed by a decrease and finally a rapid increase for all materials under the majority of applied conditions. Explanations for such behaviour have been advanced in terms of the viscoelastic response of the polymers to strain rate and temperature. Low modulus materials however showed a significant drop in wear rate under low loads above a critical velocity which is believed to be due to a transition from boundary to partial elastohydrodynamic lubrication. Generally an increase in load gave an increase in wear rate for all polymers except for UHMWPE and filled UHMWPE at a counterface roughness of 1 micrometre. These conditions have been discussed with reference to the materials response to thermal effects and counterface interactions.

GLOSSARY

A_o	: Nominal area of contact
A_r	: Real area of contact
R_a	: Average roughness value about a centre line
W,L	: Normal load
H	: Hardness
K	: Wear factor, Specific wear rate
E	: Elastic modulus
F	: Friction force
S	: Breaking stress
e	: Elongation at break
σ	: Stress
ϵ	: Strain
$\dot{\epsilon}$	: Rate of strain
μ	: Coefficient of friction
v,u	: Sliding velocity
h	: Thickness of a lubricant film
ν	: Poissons ratio
θ	: Base angle of an asperity
$\dot{W}$,WR	: Steady state wear rate
R_z	: Peak to valley roughness value
rms	: Root mean square roughness
UHMWPE	: Ultra high molecular weight polyethylene
UHMWPE/FILL	: Ultra high molecular weight polyethylene with an additive
HDPE	: High density polyethylene
LDPE	: Low density polyethylene
POM	: Polyoxymethylene
PETP	: Poly (ethylene terephthalate)
PBTP	: Poly (butylene terephthalate)
PP	: Polypropylene
PA6/MoS_2	: Polyamide 6 with molybdenum disulphide
PA6.6	: Polyamide 6.6
P(A-I)/GR	: Poly(amide-imide) with graphite
PTFE	: Poly(tetrafluoroethylene)
PPS	: Poly(phenylene sulphide)
PES	: Poly(ethersulphone)
PMMA	: Poly (methyl methacrylate)

CONTENTS

PAGE

CHAPTER 1

AIMS & OBJECTIVES

A research and development programme involving the Chamber of Mines Research Organisation and the gold mining industry has been concerned with the improvement of productivity through the provision of more advanced mining technology.

One such advance has been the introduction of hydraulically powered stoping equipment in the form of hand-held manually controlled rockdrills and also impact hammers for non-explosive rock breaking. Originally a 5% oil / 95% water hydraulic fluid was chosen for economic and environmental reasons but also for reasons of lubricity and corrosion protection. Recently this mixture has been replaced by treated mine water. The transition from an oil/water emulsion to mine service water as a hydraulic medium raises questions about the performance of various materials used for mechanical components in this new environment.

This study is concerned with the wear properties of 6 particular engineering thermoplastics (the materials are described in Section 3.8) in a water-lubricated, unidirectional sliding environment. Such conditions are likely to be encountered by the bearing surfaces between the tool holder and the body of the hydraulic rockdrill for example. Of particular interest is the response of the wear behaviour of these polymers to changes in the operating conditions within this environment. This it is hoped will add to an understanding of the mechanisms of polymer wear making possible value judgments on the selection and ultimately design of materials for particular service conditions and assist the maintenance engineer in cases of failure diagnosis. The specific aims and objectives of this research were

i) To develop a laboratory test facility which could be used to determine the unidirectional sliding wear behaviour of a number of engineering polymers from various sliding applications within the South African gold mining industry.

ii) To evaluate the relative performance of these polymers in sliding wear and to determine trends in wear rate over a range of experimental conditions.

iii) To obtain an understanding of the wear mechanisms in operation and how these relate to the observed trends.

CHAPTER 2

LITERATURE REVIEW

2.1 GENERAL INTRODUCTION

Assessments of the performance of engineering polymers with respect to one another in situations of sliding wear have been undertaken by numerous researchers, particularly in recent years. Lancaster and Evans [32] have produced a comprehensive review of the work done, as has Briscoe [12], while Bartenev and Lavrentev [9] and also Bely, Sviridenok, Petrokovets and Savkin [10] have reviewed work from the Soviet Union. Much of the information presented has been derived from laboratory work rather than in service conditions because only in the laboratory is it possible to restrict and control the many variables that play a part in wear [32].

Classification attempts are based either on the phenomena observed [4] or on the agents believed responsible for wear [19]. Most of the present review literature seems to adopt this latter course [32,12]. There appears to be consensus on the division of wear processes into four main groups viz: abrasion, fatigue, adhesive and thermal/oxidative degradation [49]. As pointed out in reference [32], there are two difficulties encountered by this formal classification. Firstly, for any one process, the detailed mechanisms of surface failure leading to debris removal depend on the mechanical properties of the material e.g. abrasive wear against rough surfaces may be due to tensile tearing for elastomers, while high modulus polymers may undergo cutting and shear under the same conditions. Secondly, there is considerable interrelationship among processes.

Briscoe [12] generalises further, dividing wear processes for polymers into two broad classes, namely cohesive and interfacial wear. Abrasion and fatigue induced by tractive stresses fall into the former category which includes mechanisms involving damage to relatively large volumes adjacent to the sliding interface, while transfer or adhesive wear and chemical/corrosive/oxidative wear make up the latter category, where frictional work is dissipated in a smaller volume and at greater energy densities [12]. Despite the difficulties with such an artificial classification, due to overlap of processes, there is a useful simplification of a complex problem [21].

An important condition for the correct approach to the qualitative examination and quantitative description of the wear mechanism is an account of the discrete nature of the contact, the actual dimensions of points of contact and the contact stresses and strains. This makes it advisable when dealing with metal-polymer pairs in contact to account for effects of time, temperature and structure [10].

2.2 WEAR MECHANISMS

2.2.1 Abrasion

For rigid polymers, the simplest physical picture of abrasive wear is one in which hard surface asperities penetrate the polymer and remove material by shearing or cutting [32]. Briscoe [12] defines the model asperity as a conical indentor of slope θ . As this cone moves through abraded material, the work dissipated is proportional to its projected area A, such that $A \simeq 2W \tan\theta / \pi H$ where W is the normal load and H the time dependent hardness. If the deformed volume is proportional to $A^{3/2}$ and the probability of this volume becoming a wear particle is K' per unit sliding distance, then v/s the wear per unit sliding distance is :

$$v/s \simeq K' \left[\frac{(2W\tan\theta)}{H\pi}\right]^{2/3}$$

For multiple abrasive contacts, the number of contacts of area A per unit sliding distance is in proportion to $A^{\frac{1}{2}}$ and total wear per unit sliding distance (z), is :

$$z = KW \tan\theta / H$$

where K is a new constant, incorporating K' and expressing the fact that only a proportion of the material undergoing deformation appears as wear debris. The important variables are therefore hardness, slope and load [12], and an essential requirement for this model is that deformation be non-elastic [32]. Halliday [33] suggests critical asperity slopes are given by $\tan\theta = C\,(H/E)(1-\nu^2)$ where ν is Poisson's ratio and C is a constant equal to 0.8 for the onset of plasticity and 2 for full plasticity.

In reality, no asperity can be perfectly sharp and all asperities must therefore have a certain radius of curvature. In general, for abrasive wear, surfaces must be rough and asperities sharp [30].

2.2.1.1 Properties Relevant to Abrasion

Ratner et al [51] postulate 3 stages involved in abrasive wear :
Plastic deformation to give a real contact area of size inversely proportional to H, relative motion against friction F = μL (L is normal load) and disruption of material involving work equivalent to the area under a materials stress-strain curve at fracture (approximately Se where S is the breaking strength and e is the elongation at break). For sliding against rough metal surfaces the product Se appears to be the most important material parameter influencing wear [32]. Fig. 2.1 shows this rough correlation for single pass wear rates plotted against $^1/Se$ for various engineering thermoplastics, emphasising the tensile nature of abrasion.

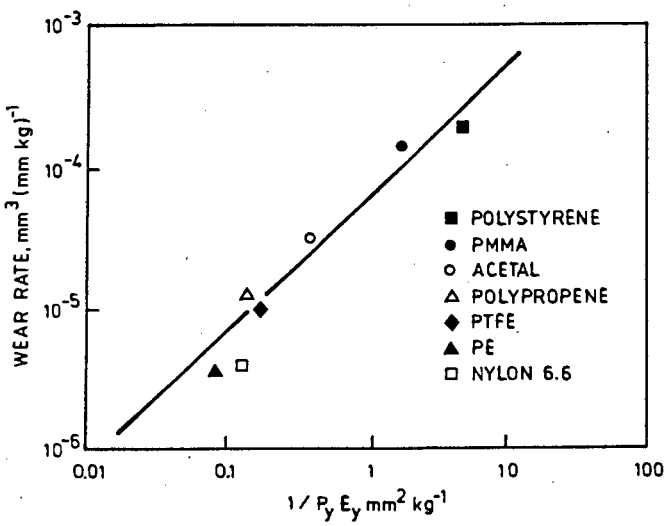

FIGURE 2.1 : Single pass wear rate vs $^1/Se$ for various polymers against a steel of counterface roughness 1.2 um R_a (after Briscoe [12]).

It should be noted that Se is determined in conventional low strain rate tests while strain rates involved in the abrasive wear process (dependent on sliding velocity) will

be of the order of 10^3 sec $^{-1}$ [32]. The existence of this correlation is then remarkable and means that Se is either independent of strain rate or that it varies with strain rate in the same way for all polymers shown. The simple theory of abrasion outlined above predicts an inverse wear vs hardness relationship. This is illustrated in fig. 2.2.

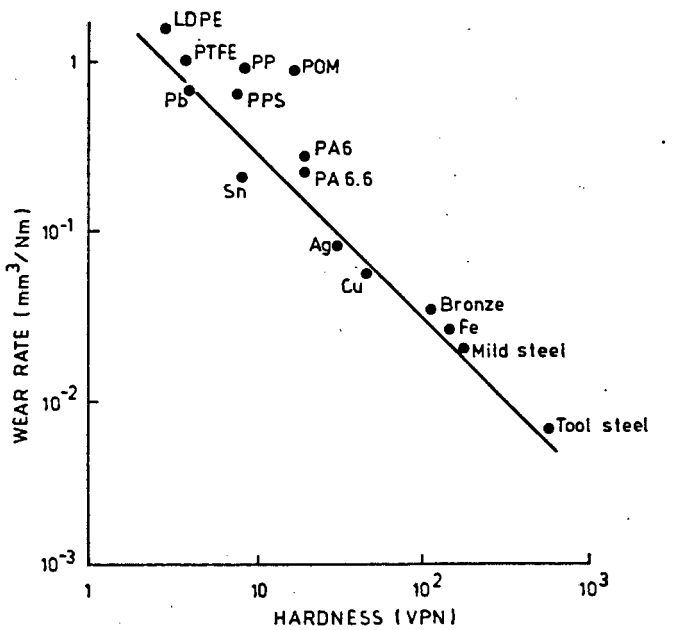

FIGURE 2.2 : Hardness vs wear rate for abrasion on 100 grade carborundum paper (adapted from [32]).

It can be seen that the correlation is far better for metals than polymers, undoubtedly because the concept of hardness has a different meaning for polymers than for metals since during deformation of a polymer by an indentor, a significant proportion of deformation is elastic and therefore the size or depth of penetration is not permanent.

Czichos [21], believes that wear volume of an abrasive process is a function of a parameter which includes the normal load F_n, the sliding distance s, the friction coefficient f and the rupture stress of the polymer σ_y. Fig. 2.3 shows the relationship.

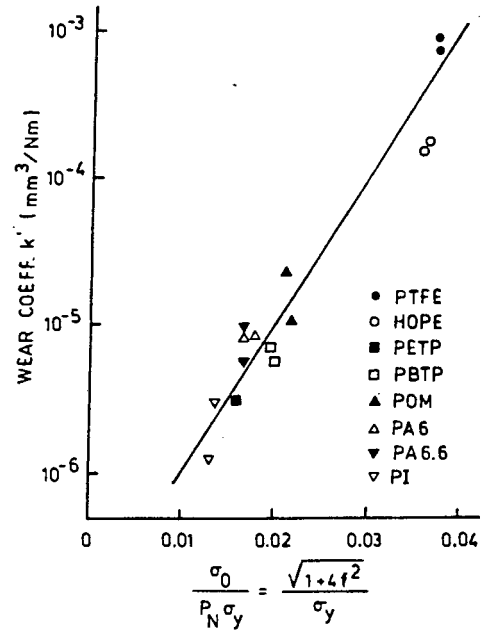

FIGURE 2.3 : Abrasive wear rate versus combined system properties parameter for various thermoplastics sliding against steel (after [21]).

σ_0 is the actual interfacial stress and is given by

$$\sigma_0 = P_N\ (1+4f^2)^{\frac{1}{2}}\ [21]$$

where P_N is the nominal normal pressure.

2.2.2 Fatigue

From the simple model for abrasion developed in the previous section, it would appear that asperity slope has an effect on the wear volume and that abrasive wear will occur for all values of θ provided that deformation is non elastic. However, Lancaster [39] showed that the wear volume versus base angle of the asperity was a linear function for soft metals but that for PMMA, the relationship only became linear for values of θ greater than 30°. Since the average slope of typical rough surfaces does not generally exceed more than a few degrees [12] another mechanism of damage must operate. With decreasing elastic modulus [32], or decreasing asperity base angle therefore fatigue processes begin to play a major role. Thus, in general, on rough surfaces with sharp asperities the wear mechanism is predominately abrasive while on rough surfaces with rounded asperities the mechanism is fatigue [30]. Neither mechanism is exclusive to a particular condition of counterface nature or polymer elastic modulus as is shown in fig. 2.4.

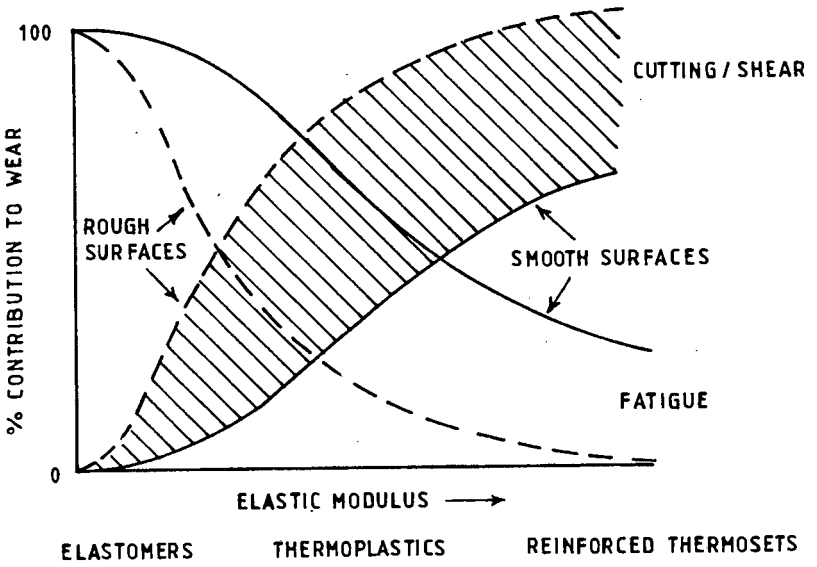

FIGURE 2.4 : The contribution of abrasion (cutting/shear) and fatigue for variations in the nature of the counterface and the polymer modulus (after [32])

Fatigue wear then is an ubiquitous process, defined as multiple deformation at separate points of real contact, leading to fracture and subsequent tearing of the material [9]. The simplest model assumes indentation of a rigid hemispherical asperity of radius r, into a smooth polymer surface under load L. Elasticity theory predicts that contact radius $a \propto (rL)^{1/3}$ and maximum stress $\sigma \propto r^{-2/3}\ L^{1/3}$. If the wear particles produced are equiaxed and similar in size to the contact diameter then the volume removed per unit sliding distance $v/s \propto a^2/n$, where n is the number of cycles to failure. This gives

$$v/s \propto r^{-2(t-1)/3}\ L^{(t+2)/3}\ [32]$$

According to Kragelskii and Nepomnyaschii [38] and Hollander and Lancaster [35], values of t derived from conventional fatigue data range from 1.5 to 3.5 for elastomers and 3 to 10 for rigid thermoplastics and thermosets. From the equation above, it can be seen that wear rates are dependent on counterface topography and that they increase rapidly with load. Recent studies involving PES sliding against smooth (0.1 μm R_a)steel, in organic fluids, under boundary lubrication, have shown that wear rates vary as $(\text{load})^{1.5}$ [6].

2.2.2.1 Properties Relevant to Fatigue

The mechanism of fatigue wear involves propagation of subsurface fatigue cracks and in this regard it has been found that superior fatigue crack propagation (FCP) resistance is exhibited by semicrystalline polymers such as nylon 6, polyacetal and poly (ethylene terapthalate). This is because crystalline polymers not only dissipate energy when crystallites are deformed but also reform a crystalline structure that is extremely strong. For example, initially amorphous PETP was shown to have strain induced crystallization in the plastic zone ahead of the crack tip [34]. Furthermore, the greatest change in FCP resistance is achieved by increasing the molecular weight in polymers such as polyacetal and polyethylene [34]. The influence of the molecular weight on the wear properties of polyethylene has been investigated, although unfortunately it has not been specified under exactly what conditions. For three different testing configurations [1], the wear rate decreases significantly as molecular weight increases. This is shown in fig. 2.5.

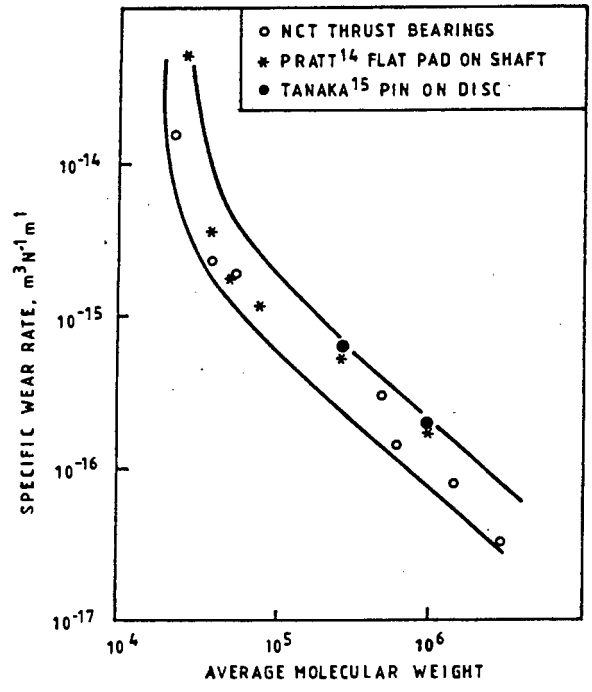

FIGURE 2.5 : Variation of wear rate of polyethylenes with molecular weight (after [1]).

Direct microscopic evidence of fatigue wear is not easily apparent, but micrographs of surface cracks in UHMWPE, which appear at a sliding distance corresponding to a sudden increase in wear rate have been published [16].

2.2.3 Adhesion

Adhesion is difficult to isolate as a unique wear mechanism because it plays a part in almost all wear processes by modifying the magnitude and distribution of the localized contact stresses, but is most significant when polymers slide over relatively smooth metal surfaces [32]. Adhesion between the polymer and the counterface is of sufficient magnitude to inhibit sliding at the original interface. Instead the junctions rupture within the polymer itself and a film of polymer is deposited on the counterface in a more or less coherent transferred layer. Subsequent traversals remove the film and displace it from the contact and the process then repeats itself [12].

The model of this mechanism [12], is divided into three sections each dealing with specific steps involved in the adhesive wear process. These are dealt with in order in the subsections below.

2.2.3.1 Adhesive Forces

The adhesive bond strength will be increased if the surface free energy of the polymer is greater. However, solids with high cohesive forces tend to be brittle and do not conform easily to a counterface (which is why polymers above their glass transition temperature (T_g) adhere more strongly). The bond strength is decreased in the presence of lubricant films [12].

2.2.3.2 Transfer

In uncrosslinked systems above T_g, the shear plane is estimated from the transfer layer thickness and is about 10nm to a few micrometres depending on the polymer and its

environment. Largely unchanged polymer is transferred with no chemical degradation but possibly morphological changes. A semicrystalline thermoplastic like HDPE shows 3 types of behaviour. At low velocities (5mm.s^{-1} or less), at room temperature, a thick (0.1 μm), fairly drawn layer is deposited at the start of sliding. After sliding has progressed about one contact diameter a much thinner (10 nm) film forms and is highly drawn in the sliding direction. This thin film only develops in what are called smooth molecular profile polymers (HDPE, UHMWPE, PTFE and POM are the only known cases). With reference to PTFE, it is recognised that the presence of a transferred layer decreases friction and wear because effective counterface roughness is decreased and because sliding occurs between oriented molecular chains of PTFE. This phenomenon occurs with other ductile thermoplastics but relatively brittle polymers like the polyesters can transfer large irregular fragments which increase the effective counterface roughness and the wear [32]. In a study where HDPE, PA and POM films were deposited on a metal substrate from solution (to stimulate friction transfer) it was found that the wear rate was decreased. This indicates that polymer films, formed on the counterface prior to sliding, improve the tribological behaviour of polymer-metal pairs [57]. The third type of transfer forms under adiabatic not isothermal conditions. Tanaka et al [58] showed that with HDPE, molten layers of about 15 μm are transferred, prior to gross melting. In the adiabatic case, the mechanical and thermal properties of the polymer will affect the film thickness by influencing the position of the shear plane. However, in steady state conditions of sliding against smooth metal surfaces, there are no well defined relationships between the wear rates of polymers and their mechanical properties. Unlike abrasive wear, neither hardness nor the product Se is particularly significant, the reason being that modifications to the contacting surfaces are induced by the sliding process [32].

2.2.3.3 Film Removal and Debris Displacement

Wear can only continue if the original layer is removed, exposing free counterface for further transfer. There is the possibility that back transfer of polymer film from the counterface to the polymer specimen occurs, a phenomenon observed by Lloyd [42]. The mechanisms of film removal are uncertain but because of orientation of the film, transverse cracking and delamination are likely [55] although chemical degradation and chain rupture may play a part. In any case, particles of polymer, immediately, after removal from the counterface, constitute wear debris and in some instances (e.g. pure PTFE) this debris may act as a lubricant while trapped within the contact. With some composites, the opposite may occur with filler particles acting as abrasives. In this case, facilitating the removal of debris (via grooves in the counterface for example) is beneficial in decreasing the wear intensity [3]. Another factor to consider in adhesive wear (or fatigue wear) is the transfer of metal to polymer [11] which occurs when the subsurface strength of the metal falls below that of the adhesive or mechanical interactions at the sliding interface [32]. The metal could be weakened by repeated contact during sliding [55] but conventional surface preparation techniques will produce locally weakened metal asperities even before sliding begins [32,42]. The metal asperities become embedded in the surface of the polymer and cause abrasive wear tracks or polishing on the metal counterface.

2.2.4 Oxidative/Chemical Wear

Polymer surfaces usually undergo oxidation or degradation during sliding [29,32] and various spectroscopic techniques - infra-red [17] or Auger [11] for example have been used to confirm this. Reductions in molecular weight of wear debris [5] may result in plasticization of surface polymer layers leading to a decrease in their elastic modulus. However, oxidation of surface layers leads to hardening and embrittlement [17] causing enhanced abrasion

(cutting) as a factor in the wear process [32]. The precise role played by chemical reactions in the overall wear process is unclear since there is no detailed knowledge of transient thermal conditions, pressure, reactants and their availability. Additional complications arise from the uncertain effects of strain activation, the catalytic effect of clean metal surfaces and the part of potentially active fillers.

2.3 COMPOSITES

Important fillers used in polymeric composite materials are carbons or graphites, inorganic glasses, transition metals and their chalcogenides and high temperature polymers like polyimide [12], which may improve the mechanical and physical properties of the polymer but not its wear properties [36]. For example, in abrasive conditions a reinforced polymer may wear faster than the pure matrix polymer. The reason for this is that although fillers increase the breaking strength (S), the elongation to break (e) is almost invariably reduced and the product Se can therefore be lower for the filled polymer. A general explanation for the mechanism of action of fillers considers the effects on transfer to and modification of the counterface. For example, solid lubricants like MoS_2 appear to transfer preferentially to the metal counterface reducing wear, whilst other fillers can prevent transfer film formation or cause metal wear [32]. An effective filler substantially increases the adhesion of the transferred layer to the counterface and hence reduces the rate of wear [54].

Examination of sliding surfaces shows an excess concentration of filler at the surface of the matrix. The filler suffers appreciable wear while standing proud of the surface, supporting a significant portion of the load and sliding over a surface lubricated with a thin film of polymer [59]. Therefore, the rate of wear is then a strong function of the filler characteristics. It has also been suggested that filler particles promote the formation of a more strongly attached transfer layer either because of mild degradation of the polymer, in the case of metal oxides, creating strong valence bonds between the transfer layer and the counterface, or because of a change in counterface roughness created by the filler which enhances film adhesion [12]. The same filler e.g.polar graphite, may decrease the wear in one polymer(e.g. PTFE [7]) but increase the wear in another (e.g. HDPE [8]).

2.4 THE EFFECTS OF SYSTEM PARAMETERS

2.4.1 Counterface Roughness

The topography of the counterface has a profound influence on the mechanism of wear [35]. On rough surfaces with sharp asperities, wear is predominantly abrasive, while on rough surfaces with rounded asperities the mechanism is fatigue. On smooth surfaces, interfacial transfer is dominant [12]. Numerous workers have found that there is an optimum surface finish to give a minimum dry wear rate of polymers on steel. Some have used mechanical grinding of the steel as a means of preparation e.g Buckley [18] who found the minimum wear rate for PE at 0.37 μm (rms), Dowson et al [27] who found the lowest wear rate for PE at 0.03 μm R_a and Czichos [21] who found the lowest wear for PA6, POM and PETP between 0.1 and 0.4 μm R_z. Other researchers have used different surface preparations. Swikert and Johnson [56] used a liquid honing method and found a minimum in wear rate at 0.1 μm (rms). In addition, it has been found by Dowson et al [27] that sliding perpendicular to the grinding direction gives a much higher wear rate than if sliding is conducted parallel to the grinding direction. They suggest that the scale, rather than the detailed nature of the asperities, is important since points around the minimum (on the wear rate versus counterface roughness graph) have been established for different loads and surface preparation methods and yet show continuity along the curve. However, it has been found that least wear corresponds to a counterface which has been prepared by blasting with rounded rather than sharp particles [56] and also that wear rates tend to decrease with decreases in average peak curvature (i.e. decreases in sharpness yet not nominal R_a, achieved by an etching technique) [30]. This information seems to contradict the previous suggestion. More recently, Tanaka and Nagai [60], using polishing with adhesive cloths and buffing with alumina powders, have found a minimum in the wear rate for LDPE and HDPE at 0.025 μm R_a with rapid increases below 0.01 μm and from 0.025 - 0.2 μm, followed by more gradual increases above 0.2 μm. They suggest that wear is due to transfer below 0.025 μm while the rapid rise in wear rate above this value is due to transfer and abrasion. The gradual rise in wear rate above 0.2 μm is predominantly due to fatigue and partially due

to transfer. This is shown in fig. 2.6(a) and (b) below.

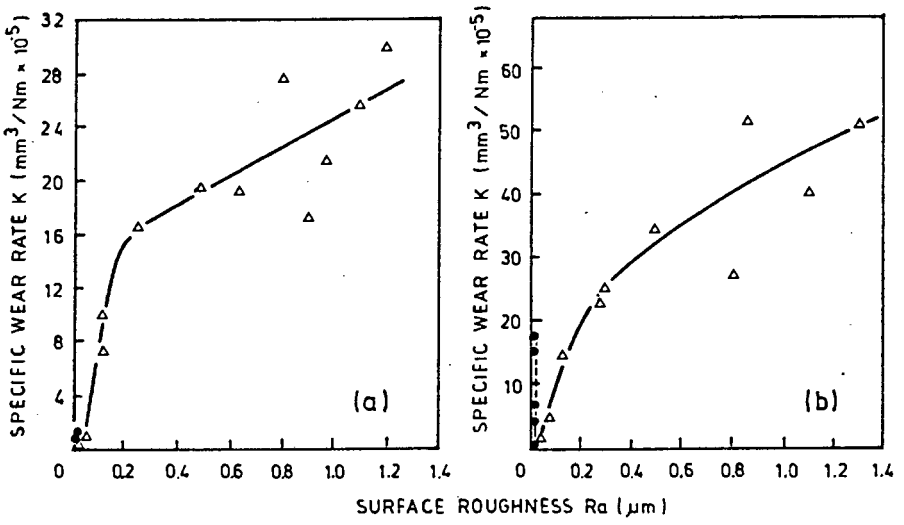

FIGURE 2.6(a) & (b) : Variation of specific wear rate for HDPE and LDPE respectively with counterface roughness R_a. The closed circles are obtained on polished surfaces. (After [60]).

Later work [61] involving increased sliding speed and surface melting shows similar trends, leading to the conclusion that wear on a rough counterface appears to be caused predominantly by abrasion rather than fatigue.

In the presence of water, transfer film formation is largely inhibited and this results in a much more pronounced effect of counterface roughness on the wear factor.

Dowson et al [28] found that above 0.01 μm R_a, the "wet" wear factor exceeds the dry wear factor for UHMWPE. Below this value the reverse is true. The transfer film was seen to build up in thickness as the counterface became smoother, exceeding the R_a at about 0.1 micrometres. This suggests that the transfer film thickness relative to R_a is responsible for the minimum dry wear factor.

In the case of thermoplastic composite materials it has been found that a minimum wear rate exists for an initial counterface roughness of 0.3 - 0.4 μm when using glass/carbon fibre and PTFE filled PA66 against 440 and 304 stainless steel [64]. The counterface topography is modified by the abrasive action of fillers, which

enhances transfer film adhesion [12]. When carbon is used as a filler, only those carbons which abrade the counterface produce viable composites, perhaps because the abrasion process may clean the counterface and ensure close contact between the metal or oxide and the polymer film [13] and also because the optimum surface finish for film adhesion may be produced [12]. However, Lancaster et al [32] state that many fillers are abrasive to the metal counterface and can prevent transfer film formation or cause metal wear. Correlations between counterface topography and wear of polyimide filled with PTFE and CF_x powders have been found [50] in that wear increased with average roughness or asperity slope and decreased with an increase in number of peaks and radii of curvature. Tanaka and Yamada [62] found that the wear of POM and PTFE based glass/carbon fibre composites were virtually independent of the counterface roughness. If solid lubricants or bronze fillers were used then wear rates increased markedly beyond a characteristic roughness. The variation in wear rate with roughness is strongly controlled by transfer [62]. In the presence of water, wear rates are higher for those composites that, in dry conditions, rely on transfer to produce a low rate of wear, suggesting that the abrasive action of fillers on counterface polishing could exert a dominant influence on wear in water lubricated conditions. Abrasive fillers can reduce wet wear rates to values not very different from those in dry conditions with or without abrasive fillers. This means that by selecting fillers with the correct degree of abrasiveness, polymer composites can be formulated whose wear properties remain insensitive to the presence of water [32].

2.4.2 Load/Pressure

The simple models of wear developed in sections 2.2.1 and 2.2.2 show that in the isothermal case, where frictional heating and softening can be neglected, the dependence of wear rate on load is linear for pure abrasion and a power function (wear rate $\propto$ (load)^x where $x>1$) for pure fatigue wear. Simple adhesive wear theories predict direct proportionality between wear rate and load only when changes in load do not induce changes in any other variable affecting wear such as the temperature [32]. Thermal softening will result in a loss of proportionality and a rapid rise in wear rate, as shown in fig. 2.7.

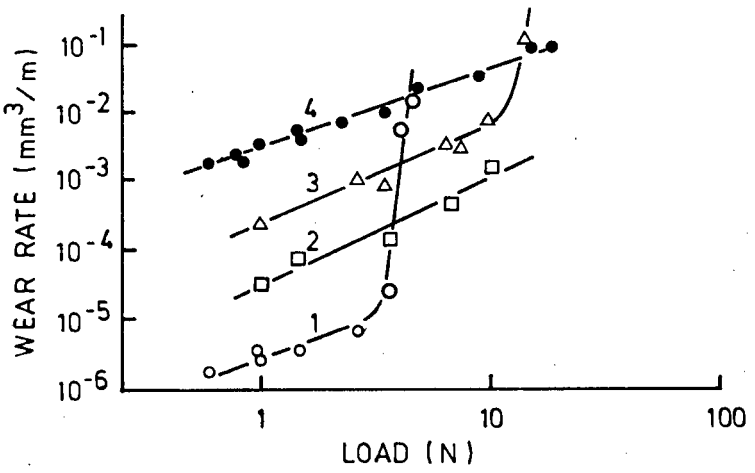

FIGURE 2.7 : Variation of steady state wear rates with load for 1-LDPE, 2-PA6, 3-PMMA, 4-PTFE against 0.15 μm R_a mild steel (after [32]).

The critical load above which thermal softening occurs can be increased by gamma irradiation which for LD-, HD- and UHMW polyethylenes introduces cross linking and inhibits melting [45,53] or which causes chain scission and more effective chain packing (or higher effective crystallinity) in PTFE [14]. Watanabe and Yamaguchi [63] have found that there is a minimum in the wear rate versus load curve for PA6 and have attributed this to the influence of the interfacial temperature on the position of the shear plane (fig. 2.8). In the area of the minimum, the shear plane exists at the nylon/metal interface, minimizing wear loss, while on either side of the minimum the shear plane exists within the oriented molecular layers of the nylon itself which increases wear loss, but decreases friction.

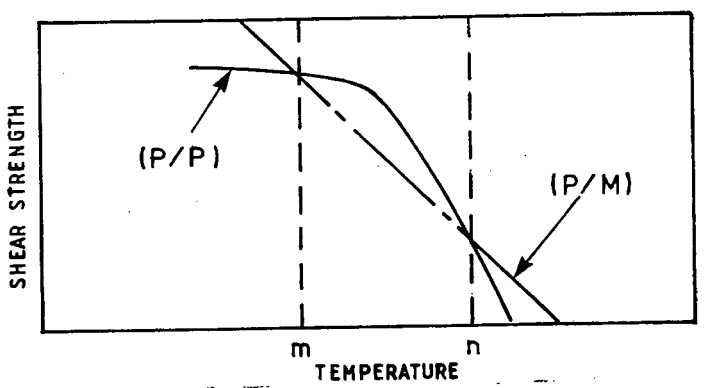

FIGURE 2.8 : The shear strengths of the polymer/metal interface (P/M)and the polymer bulk (P/P) during temperature increase (After [63]).

Recent work involving the load dependence of wear in polymer based composite materials has been carried out. Graphite fibre filled nylon shows a linear dependence up to 5 MPa under abrasive wear conditions [46]. PTFE + graphite filled poly(amide-imide) copolymer shows a region of virtual independence followed by a linear dependence above a critical load [37], which is shown in fig. 2.9

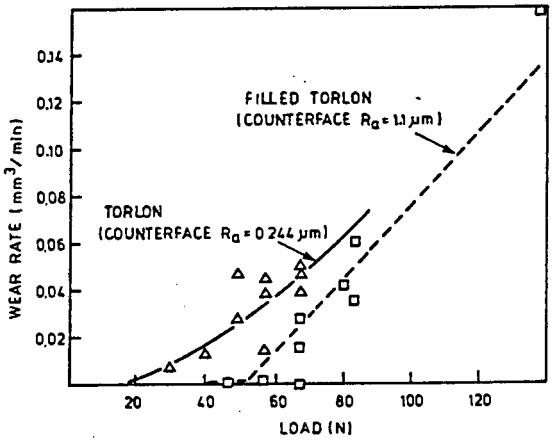

FIGURE 2.9 : Variation of wear rate of Poly(amide-imide) copolymer with load when sliding against a steel disk at 1 m/s. (After [37]).

Lhymn [43] has shown that for nylon/glass fibre composites sliding on abrasive paper, the specific wear rate decreases as the load increases at low sliding velocity while the reverse is true at high sliding velocity. The specific wear rate of acetal/glass-fibre sliding on a steel plate decreases as the load increases, especially at high sliding velocity. At low sliding velocity the specific wear rate versus load curve initially rises to a distinctive peak owing to material softening and then becomes constant probably because of the attainment of abundant molten film formation. At high speeds it is probable that degradation of polymer occurs and the specific wear rate decreases owing to the lubricating effect of the softened polymer film at the contact spots [43].

2.4.3 Sliding Speed

Speed is a particularly important system parameter because of its role in the viscoelastic response to stress and the generation of frictional heat. With rigid "engineering" polymers, variations in

wear rate with speed are complex because the mechanisms of wear usually include both deformation and interfacial components [15] and transfer can also play an important role. Therefore, no unique trend between wear rate and speed is to be expected and wear rate - speed relationships have shown maxima, minima or little variation depending on materials and conditions [58,40]. In dry sliding conditions thermoplastics show an increase above a critical speed associated with softening or melting and the magnitude of this speed is dependent on the thermal conductivity of the counterface [32]. Less information is available about lubricated polymer wear. The main problem is that as speed increases there is an increasing tendency toward load support from hydrodynamic or elastohydrodynamic lubrication on an asperity scale or via geometric wedge formation [41]. Polymers are particularly susceptible to this because of their relatively low elastic moduli [20]. Geometric wedge formation is most likely to result from elastic deflections of the polymer or its support system and will thus depend on the geometrical configuration of the contact and the stiffness of the loading assembly. Prediction of conditions for which fluid film formation ceases to be significant (i.e. boundary lubrication) is therefore not easy [25].

For polymer composites the situation is very much unknown but data for glass fibre and carbon fibre reinforced PBTP generally follow the theoretical pattern of fig. 2.10 [20].

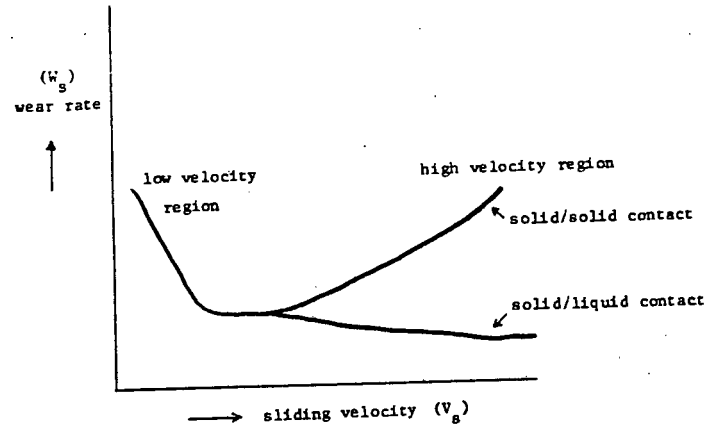

FIGURE 2.10 : Theoretical curve of specific wear rate vs sliding velocity (after[20]).

2.4.4 Lubrication

Any material that reduces friction, wear or surface damage of sliding components may be called a lubricant. A lubricant functions by preventing or mitigating the formation of strong adhesive junctions between the high spots, or asperities, on opposing surfaces. This is accomplished by one or more of the following mechanisms :

a) The complete separation of surfaces by a sufficiently thick hydrodynamic or elastohydrodynamic (EHL) film so that the tops of the opposing asperities do not come into contact.

b) The formation of a surface film by either physical or chemisorption of a gas (vapour), liquid or compounds dissolved in a liquid.

c) The formation of a tenacious surface film by chemical reaction of the lubricant with the (metal) surface.

d) Prior treatment of one or more of the surfaces with some material to form a tightly adhering solid film or coating.

Thus, the majority of gases, liquids and solids will possess some lubricating ability under certain conditions [52].

2.4.4.1 Boundary Lubrication

In this regime the load is carried almost entirely by deformation of the solid asperities and the physico-chemical solid-lubricant interactions determine the friction and wear behaviour of the system. Wherever a fluid film is not maintained between sliding surfaces, the contacting 'boundaries' of the bodies in relative motion suffer wear, usually including some transfer of material [23]. The main purpose of a boundary lubricant is to interpose between the moving surfaces a film that is able to reduce the amount of direct solid/solid interaction and that is itself easily sheared [24].

2.4.4.2 Hydrodynamic and Elastohydrodynamic Lubrication

A simple definition of hydrodynamic lubrication is the build up of a continuous fluid film by the wedging action produced by two non-parallel surfaces having relative motion which is sufficient to support an applied load without causing metal-to-metal contact. The load capacity will be greater at higher speeds and with higher values of viscosity [22]. In most common applications where the interacting surfaces are assumed to be smooth, rigid and inflexible, load support can be attributed to the wedge effect. However, if one (or both) of the sliding members have viscoelastic properties, it is clear that relative stretching of the material causes an additional increment in load support [48]. During lubrication of the soft and flexible surfaces of viscoelastic and elastomeric materials, the elastic deformation of the surfaces must be taken into account. This is elastohydrodynamic lubrication (EHL). When fluid lubricants are present, polymers (low modulus materials) exhibit elastohydrodynamic film formation more readily than metals [32].

2.4.4.3 Partial Elastohydrodynamic or Mixed Lubrication

If, under EHL conditions, the lubricant viscosity or the velocity decreases, or the load increases, the lubricant film is thinned and separation of the surfaces decreases. Asperity contact interactions occur and partial EHL or mixed lubrication occurs, where the load is now carried partly by the fluid film and partly by the contacting asperities. If the lubricating conditions operating in this regime move to the left of the Stribeck curve (fig. 2.20), asperity interaction increases, film thickness decreases down to some monolayers or below, and boundary lubrication processes prevail [48].

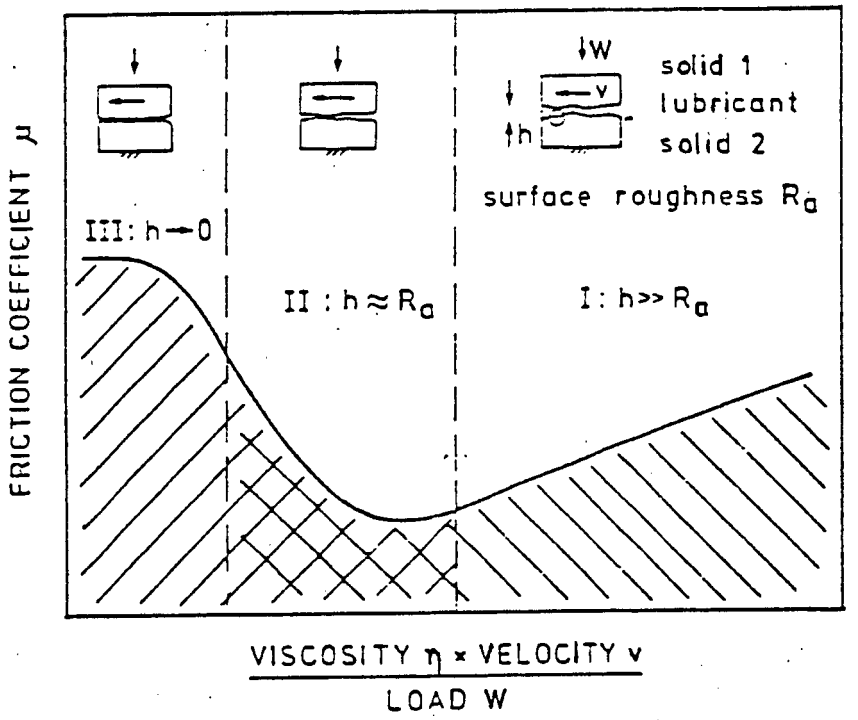

FIGURE 2.11 : The Stribeck curve. Regime I - hydrodynamic lubrication (and elastohydrodynamic lubrication). Regime II - partial EHL or mixed lubrication. Regime III - boundary lubrication. (After [22]).

It has been found [26], that the velocity U_{bm} at the transition from boundary to mixed lubrication is proportional to :

$$P_e r(1 - cP^{1/4})/u$$

where P_e = external pressure
r = surface roughness
P = unit load
u = lubricant viscosity
c = constant of proportionality

CHAPTER 3

DESIGN AND EXPERIMENTAL TECHNIQUE

3.1 DESIGN RATIONALE

The purpose of conducting these sliding wear tests was to obtain data on the performance of specific materials in conditions of unidirectional sliding wear. This was to satisfy a need for information regarding the in-service behaviour of certain components in use in tribological applications in the South African gold mines.

In order to achieve these objectives a laboratory test was needed which would attempt to simulate the operating conditions of hydraulic stoping equipment, notably a hand-held rockdrill, and yet be sufficiently flexible in the control of experimental parameters. This would allow a wide range of conditions to be explored, helping to satisfy two main objectives. The first main objective would be to rank materials in terms of wear resistance in conditions that simulate the essential characteristics of the application. The second objective would be to contribute to an understanding of wear mechanisms with a view to optimising the use of existing materials, assisting in failure diagnosis and aiding the development of new materials.

3.2 SELECTION OF VARIABLES

A number of operating variables are known to affect the wear behaviour of polymeric materials, inter alia :

i) The nature of the counterface in terms of its surface roughness.

ii) The bearing pressure at the sliding interface.

iii) The relative sliding speed of the two surfaces in contact.

iv) The presence of a lubricant such as water.

A laboratory wear testing machine was therefore sought which would allow monitoring of and close control over these variables.

3.2.1 Sliding Velocity

The sliding components of the hydraulic stoping machines presently in use encounter a range of sliding velocities, typically between zero and 10 $m.s^{-1}$. The rotating tool holder at the front end of the rockdrill operates at 200 rpm, which, considering the dimensions of the shaft and the ratchet mechanism, gives speeds of sliding at the bearing surface of between zero and 0.6 $m.s^{-1}$.

3.2.2 Pressure

Within the body of the hydraulic drill, seals must contain pressure differentials of between zero and 35 MPa. However, at the contacting surfaces of the rotating shaft, the pressure is not known, and is unlikely to be constant. It is likely to be fairly small (in the region of 1 MPa say) for most of the time, since all that is required is location and support of the shaft. However, it is possible that pressure spikes of much higher magnitude will be encountered in practice as a result of side loading of the drill and temporary misalignment of the tool holder.

3.2.3 Surface Roughness

The surface roughness of the sliding steel components in use varies considerably, with preparations such as surface grinding or chrome plating and liquid honing giving rise to values in the range of 0.2 - 0.8 micrometres R_a. The polymer bearing and seal surfaces have roughnesses of approximately 1.8 micrometres R_a.

3.2.4 Lubrication

The hydraulic stoping machines were originally designed to operate using mineral oil lubrication and have since been modified to run on 5% oil, 95% water emulsion. The latest efforts in design have looked at the possibility of eliminating the use of mineral oil altogether, with the equipment operating in treated minewater alone. The quality of mine service water used in the South African gold mines is very variable in terms of chemical constitution and suspended solids, with entrained abrasive particles often too small

to be filtered out by conventional methods. High concentrations of chloride and sulphate ions are usually present as a result of high dissolved solids concentrations.

As a typical example, the analysis of a sample of water from a far West Rand mine, taken on 20/03/85 appears below in Table 3.1.

TABLE 3.1 : Analysis of a sample of treated minewater

pH Value	6.8
Total dissolved solids	2360
Total suspended solids	34
Total hardness (as $CaCO_3$)	881
Chloride, Cl	226
Sulphate, SO_4	816
Nitrate, NO_3	458
(Values expressed in ppm where applicable)	

3.2.5 Summary

The criteria for the selection of a design for the wear testing apparatus falls into two broad categories, as laid out in the sections above. Firstly, using specimen geometries that are practical in terms of size and ease of machining, it was envisaged that material couples would be tested over a fairly broad spectrum of experimental conditions, involving monitoring and control of sliding speeds, pressures, counterface roughnesses and lubricant. The data gathered thereby, together with examination of the sliding surfaces, would give a general idea of the wear characteristics for the different materials in terms of relative wear performances and the wear mechanisms in operation. Secondly, it would be useful if the actual operating conditions in practice (in this case, in the hand held rockdrill) lie within the range of experimental parameters used. This would give the study a practical usefulness by allowing at least qualitative predictions to be made about the performance of components in practice.

3.3 THE TESTING SYSTEM

The basic wear testing system developed for use in conducting this research project is based on a modified vertical drill. A hollow rotating steel counterface, which would allow a continuous supply of fresh lubricant, was allowed to rest under static load on top of a disc of the polymeric material to be tested. The steel counterface is akin to a drill bit with a flat face of some specified roughness. The polymer disc is held stationary in a clamp so that a wearing action takes place between the steel and the polymer in the presence of a pressure fed lubricant travelling down the centre of the spinning steel shaft and emerging at the sliding interface. Figure 3.1 is a schematic representation of the spinning steel counterface bearing down on the polymer disc specimen.

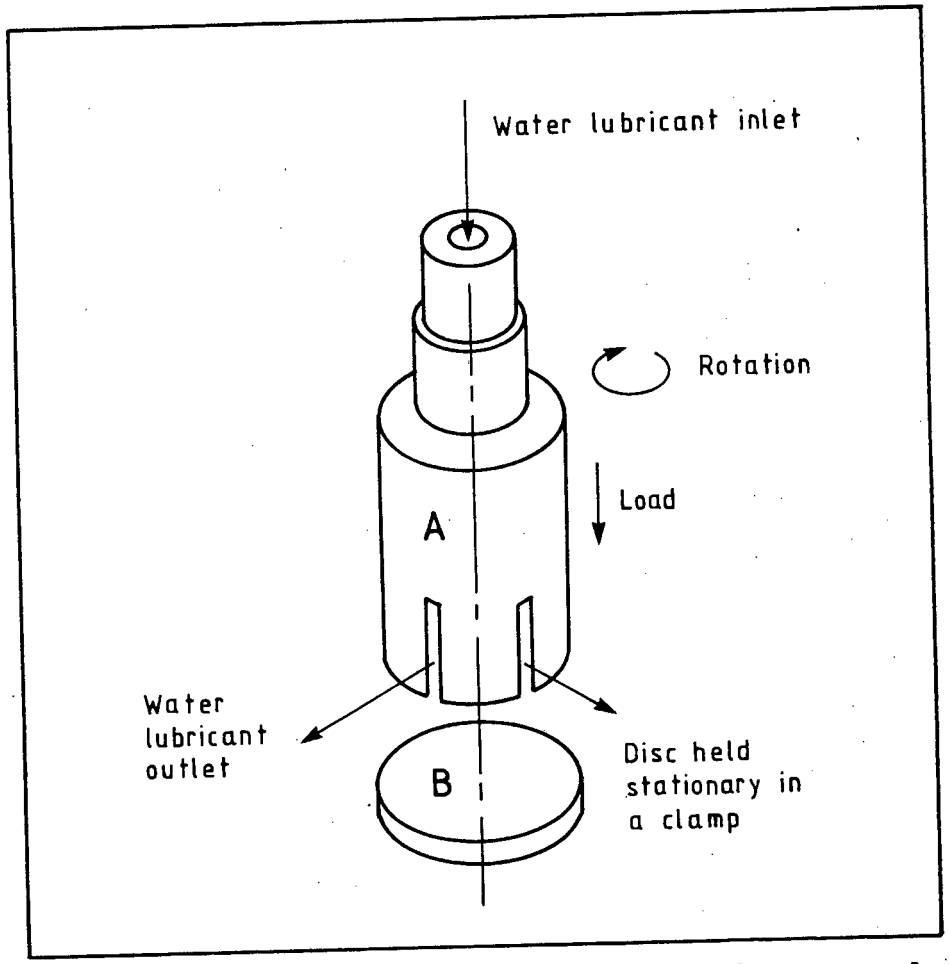

FIGURE 3.1 : The basic testing system. A: steel counterface; B: polymer specimen.

The counterface is screwed into a chuck which in turn is screwed into the spindle of the drill. The polymer disc specimen is seated in a recess in an AISI 431 steel block with relative movement between specimen and block prevented by a brass plate which clamps down over the disc. There is a hole through the brass plate to allow contact between the steel counterface and the polymer disc. This block is held to the turntable by lateral clamps, as seen in fig. 3.2.

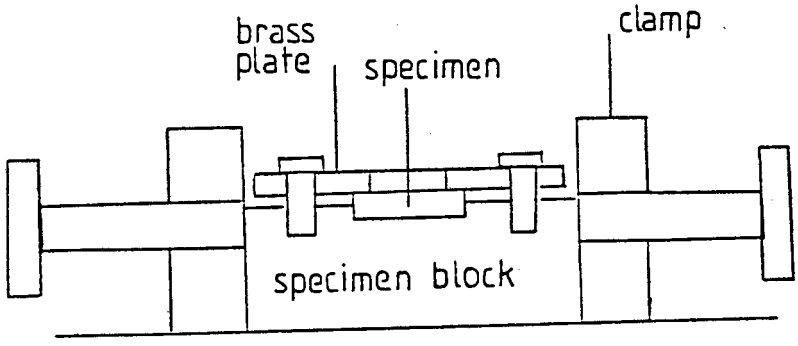

FIGURE 3.2 : The clamping arrangement for polymer specimens.

3.4 SPECIMEN GEOMETRY AND PREPARATION

3.4.1 The Rotating Counterface

The rotating counterface specimens (or "drill bits") were machined from AISI 431 stainless steel rod of ¾inch (19.05mm) diameter. The basic design allows for lubricant to flow down the centre of the bit and out through 4 symetrically placed (90° apart) slots in the wall of the hollow bit. The edge that each slot makes through the thickness of the wall was rounded off using a fine grade dressing stick, for reasons explained in the "Preliminary Tests" section. A detailed drawing of the specimen geometry appears in Appendix B. After machining, the specimens were heat treated in the following manner:

A ceramic coating (FOSECO ISOMOL 100) intended as protection against oxidation and usable up to 1600°C was applied to the specimens as a slurry of zirconia based particles in methanol. This coating was applied in layers by repeated dipping in the slurry and oven drying until the final thickness of the coating was approximately 2 mm. The specimens were then soaked at 1010°C for 45 minutes, oil quenched to room temperature (approx. 20°C) and tempered at 260°C for one hour. The resulting hardness, measured on an ESEWAY type SPVR.2.M universal hardness tester was 452-485 HV30 (46-48 HR_C). A similar treatment was used for this material in other sliding wear tests [42], and was said to be that which is used for AISI 431 machine components. The treatment improves the fatigue strength and impact toughness as well as the corrosion and wear resistance of the steel.

The final surface roughness was obtained using a mechanical surface grinder and could be varied between 0.1 and 1.0 micrometres R_a by changing the grit size of the grinding wheel, the feed rate and the depth of cut. All 6 specimens needed for one set of tests (6 individual tests) were ground at the same time while being held in a specially made jig (fig. 3.3). This was done because great difficulty was experienced in reproducing a particular surface finish.

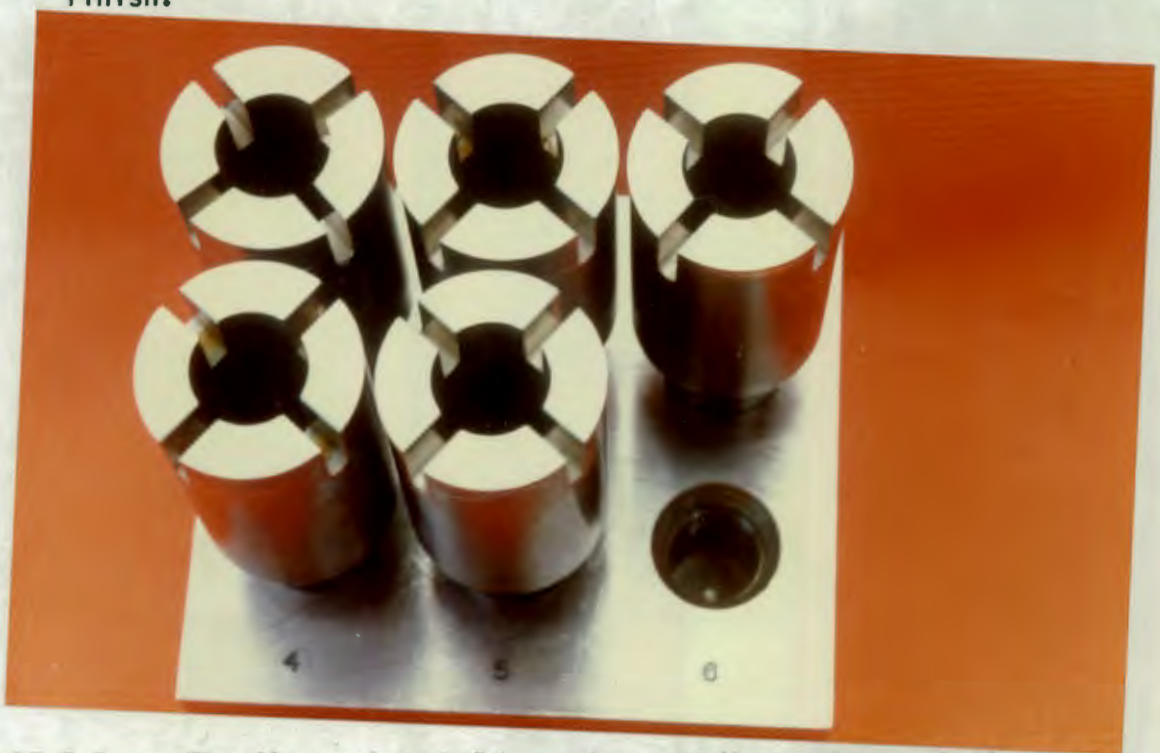

FIGURE 3.3 : The jig used to hold specimens while surface grinding.

A Rank Taylor Hobson TALYSURF 4 surface profilometer was used to monitor the surface finish and the mean of 6 readings at right angles to the grinding direction on each of the surfaces was used as the representative value for a particular specimen. The lay of the surface after grinding was directly across the circular bit face as shown in fig. 3.4 below and roughness measurements were taken on those segments of the face where the lay is at 90° to the tangent of the circumference.

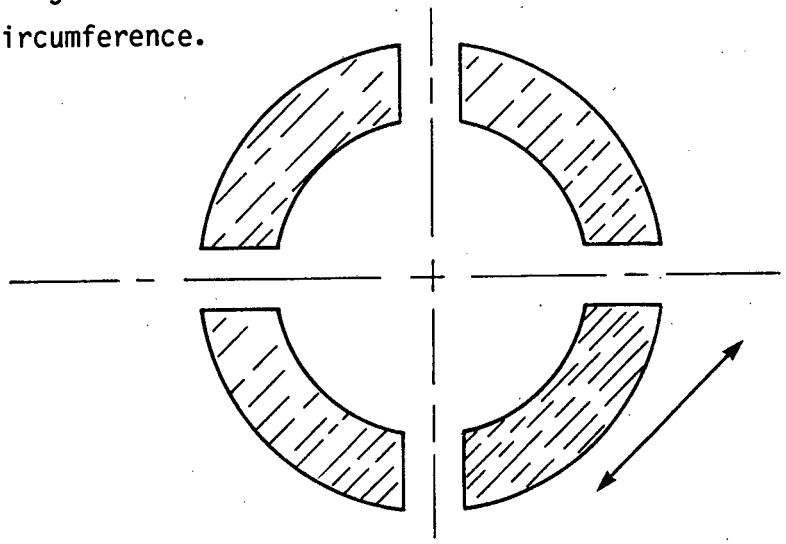

FIGURE 3.4 : The cross-ground surface of the counterface with arrows showing the grinding direction (drawing not to scale).

After machining and surface grinding the bits were demagnetised to allow any metallic particles produced to be removed by the subsequent ultrasonic cleaning in Arklone (a commercial degreasing solvent).

3.4.2 The Stationary Polymer Discs

The stationary polymer disc specimens were machined from various bar and hoop shaped stock. If bar stock was extruded then the discs were machined with their thickness parallel to the extrusion direction. This means that sliding at the polymer/metal interface takes place perpendicular to the extrusion direction. All specimens were taken from the core of the rod (fig. 3.5) in order to minimize possible anisotropy effects [42]. In the case of cast or sintered stock, the discs were machined from the centre of the casting with their faces parallel to the mould wall (fig. 3.5). This ensured that the structure was homogeneous through the thickness of the disc

compared to mould dimensions) and across the diameter of the disc (comparable to the thickness of the moulded stock). Bar stock was chosen for ease of machining and hoop stock was used if it was the only available geometry.

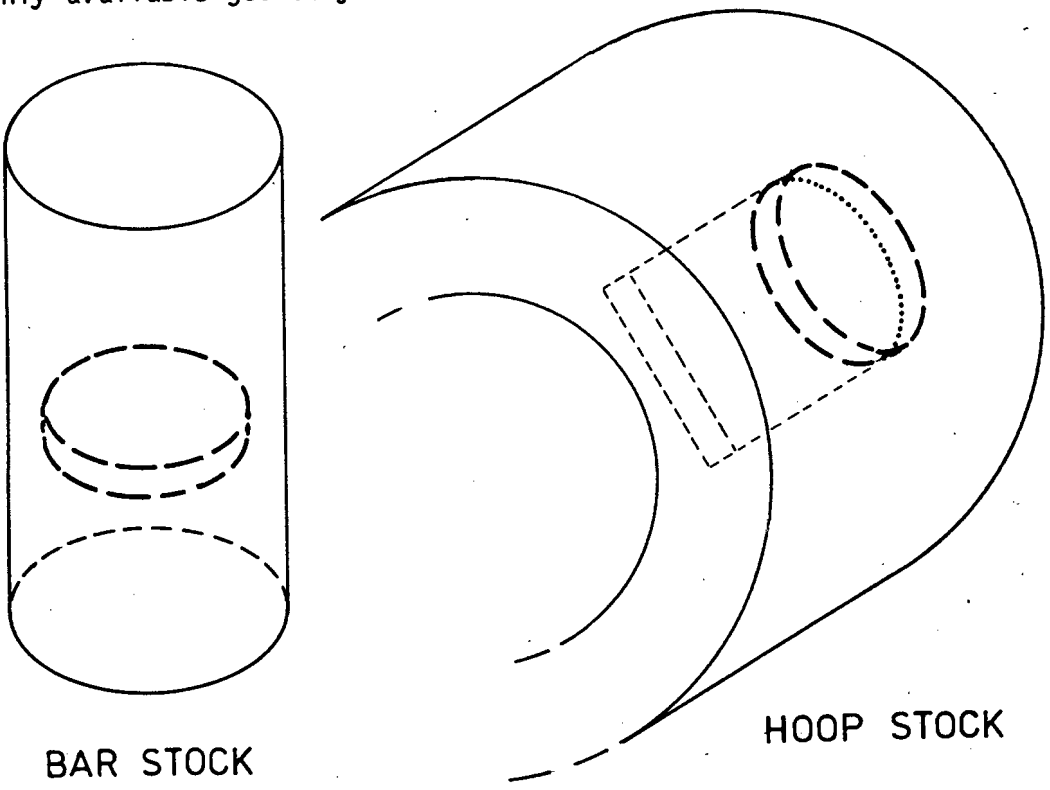

FIGURE 3.5 : Schematic view of how specimens were machined from stock.

A detailed drawing of the polymer disc geometry appears in Appendix B. A chamfer was put on the lower edge to facilitate insertion into the specimen holder, while the upper surface was cleaned on the lathe with a cutting tool. This gave the surface a circumferential lay with a roughness that varied between 0.8 and 2.2 micrometers R_a. This variation was however not significant since, as will be explained in the "Experimental Procedure" section, all specimens were "run-in" against the counterface before steady state wear rates were calculated.

After machining, the polymer specimens were ultrasonically cleaned in ethanol to remove any dirt from the machining process. Ethanol was chosen as a cleaning solvent because its low surface tension ensures complete wetting of the polymer during cleaning, while it is not reactive to any of the polymer materials used.

3.5 DESCRIPTION OF THE LABORATORY WEAR TESTING RIG

3.5.1 General Design

The laboratory wear testing rig used was based on an Arboga 2512 GM pillar mounted machine (fig. 3.6) with specifications as listed in Table 3.2. This rig was used originally for investigations into wear behaviour of diamond impregnated drill bits when sliding against various ceramic materials [47].

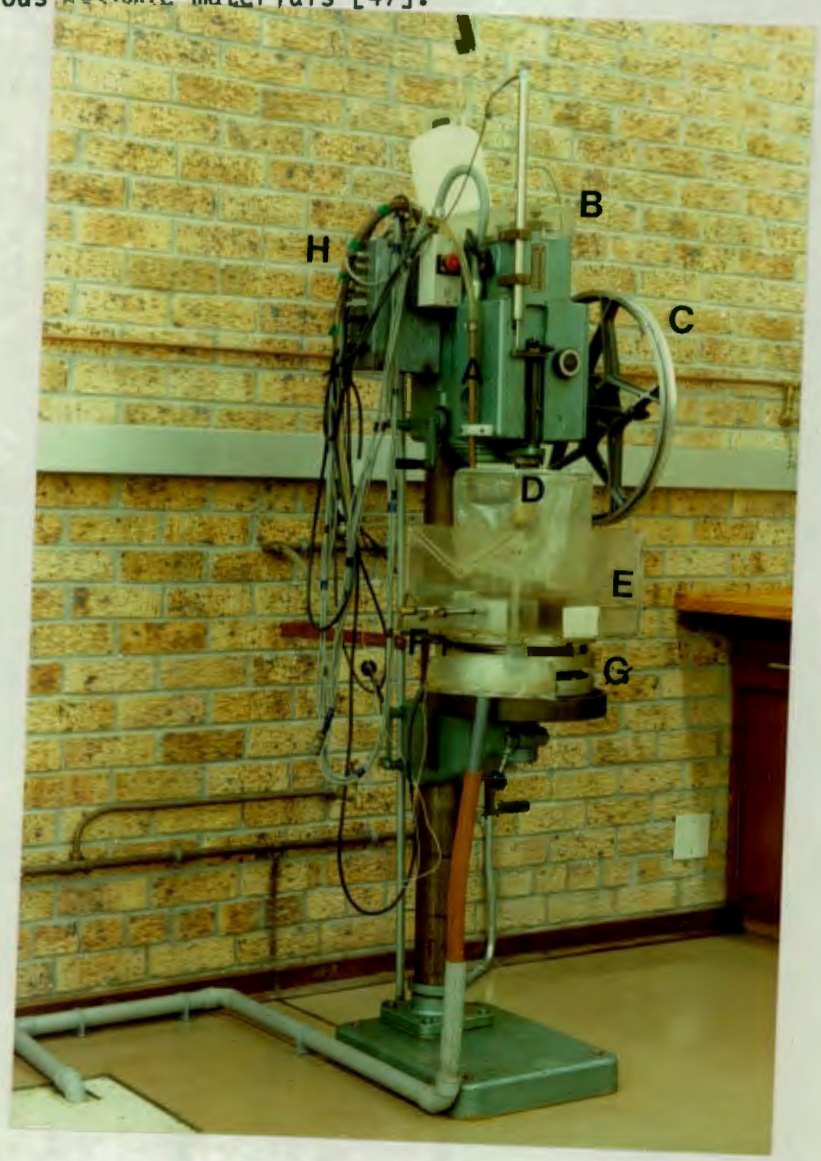

FIGURE 3.6 : The modified Arboga machine.

A : Water feed hose
B : External gearing
C : Manual feed system
D : Drill shaft
E : Splash box
F : Specimen clamp screws
G : Turntable discs
H : Electronic monitor

TABLE 3.2 : Drilling rig specifications.

Maximum spindle speed	3500 rpm
Motor	1kW, 3 phase, AC
Spindle internal taper	Morse no. 3
Maximum quill movement	110mm
Maximum distance from spindle nose to table	900mm

3.5.2 Loading System

A 460mm diameter cast light alloy motorcycle wheel with the rim turned down was fitted, via a shaft and a rack and pinion type connection to the drill shaft. A steel cable was wound around the wheel and passed to a PTFE pulley above the rig. The rig and pulley were securely mounted on the laboratory floor and wall respectively. A hook, attached to the end of the cable could carry different weights which would be transmitted via the cable/pulley/gearing system into a load or downward thrust along the axis of the drill shaft. It was found that the most convenient way of applying the load was by suspending 10 litre plastic water containers, filled to the desired levels, from the hook. A load cell with an activation voltage of 8.762 V DC was situated below the turntable. The calibration equation for the load cell is:

LOAD (kgf) = OUTPUT VOLTAGE X 1000 X 0.3332/ACTIVATION VOLTAGE

With the aid of the electronic monitor, a 3497A HP data acquisition and control unit and an HP 85 microcomputer the load can be set and the nominal contact pressure between specimen and counterface calculated using:

PRESSURE (MPa) = LOAD (kgf) X 9.8/NOMINAL CONTACT AREA (mm^2)

The mass of the drill chuck, shaft etc. and the specimen geometry causes an inherent minimum applied pressure for the unweighted system which was just below 1 MPa. It was decided therefore to use a slightly filled plastic container to bring the minimum pressure to a realistic value of 1MPa. The maximum pressure is limited by the monitoring equipment and the specimen geometry. With the KYOWA LC-500 KF load cell at a 500 kgf capacity, the maximum nominal contact pressure allowable would be 25 MPa.

3.5.3 Rotational Speed Settings

A 1 kW, 3 phase, AC motor, which turns at 2790 rpm is coupled to the drill chuck through a system of spur gears. The gears can be manually changed or repositioned to vary the frequency of rotation of the drill chuck. The drill bit specimen geometry, together with the fixed rotational frequencies gave a finite series of peripheral or tangential surface velocities at the face of the bit. A list of these rotational frequencies and their corresponding average tangential velocities appears in Table 3.3 below. The average tangential velocity for each frequency is found by taking the mean of the inner and outer peripheral velocities and allowing for the effect of the four symmetrically placed slots which act as waterways. A detailed explanation of the calculations appears in Appendix A.

TABLE 3.3 : Rotational frequencies and corresponding velocities.

ROTATIONAL FREQUENCY (rpm)	AVERAGE TANGENTIAL VELOCITY ($m.s^{-1}$)
200	0.1296
260	0.1685
345	0.2236
435	0.2819
560	0.3629
750	0.4861
950	0.6157
1280	0.8295
1640	1.0629
2080	1.3480
2800	1.8146
3500	2.2683

3.5.4 Lubrication System

Water from the mains supply was used as the lubricant and coolant. A cylindrical, perspex NIXON flowmeter with a rider, was used to monitor the flow in litres per hour and a FERRIS pressure gauge gave a reading of the line pressure in kPa. The flow rate was controlled by adjusting a tap. The water flowed down the drill shaft out across the polymer specimen and drained off through a hole in the base of the splash box. An analysis of the laboratory water from the mains connection appears in Table 3.4 below.

TABLE 3.4 : Analysis of a sample of laboratory water.

pH value	7.2
Total dissolved solids	100
Total suspended solids	20
Total hardness (as $CaCO_3$)	60
Chloride, Cl	25
Sulphate, SO_4	12
Nitrate, NO_3	0.7
(Values expressed in ppm where applicable)	

3.6 EXPERIMENTAL PROCEDURE

The wear rates of the polymers were calculated from weight loss (converted to volume loss by dividing by the density of the polymer) versus sliding distance relationships. This meant interrupting a test at regular intervals to take the weight measurements which led to the adoption of the following standard testing procedure :

Starting

a) The polymer disc is placed chamfered side down in the recess in the clamped steel block.
b) The brass plate is fitted and screwed down over the polymer disc.
c) The counterface is screwed into the chuck on the drill shaft.

d) Water is turned on and the counterface lowered onto the specimen. The flow rate of water is set at 400 l/hr.

e) The gearing is checked to ensure that the correct spindle speed has been selected.

f) The time is noted and the rig switched on.

Stopping

a) After the test has run for the required time, the counterface is raised and the rig switched off.

b) The water is turned off.

c) The brass plate is unscrewed, the specimen removed and rinsed off in ethanol.

d) The specimen is ultrasonically cleaned in ethanol, dried and weighed to 0.1 mg accuracy.

e) If the test is to continue then the specimen is clamped in the holder and the testing procedure repeated. If the test is complete then the counterface is unscrewed, rinsed in ethanol, dried and stored in a dessicator with the polymer specimen. After examination on the scanning electron microscope the counterfaces were reground for re-use in the next wear test.

3.6.1 Test Duration

The tests were run until a linear volume loss versus sliding distance relationship was attained. For rougher counterfaces it was found that testing intervals of 233 m sliding distance were suitable, with the steady state wear rate achieved afer one interval of testing. For this reason, all specimens were run-in against their respective counterfaces for a period equal to one testing interval before testing began. Testing within the linear portion of the curve was extended until at least six points within this region had been obtained. A straight line was fitted to the data points by means of a linear regression computer programme, and the gradient of the line taken as the steady state wear rate representative of the particular conditions of the test.

3.6.2 Correction for Water Absorption

Water absorption tests were conducted on all the materials tested and weight increases measured at regular intervals. Cleaned polymer discs were placed in beakers of tap water for a duration and removed ultrasonically cleaned in ethanol, dried and weighed. This treatment was identical to that which an actual wear specimen would receive and therefore consituted an effective 'control' experiment. Initially, weight increase was monitored every half hour and after 4 hours, every 4 hours thereafter. This was because with rougher counterface wear tests half an hour was the maximum interval used, while with smoother counterface wear tests the time interval used was four hours. The percentage increase in weight due to water absorption after each interval could then be used to correct weight loss values due to wear plus water absorption in the actual wear tests.

3.7 PRELIMINARY TESTS

The original specimen geometry was slightly different from that mentioned in Section 3.3. The original counterfaces were 10 mm in diameter with a 6 mm diameter hole through the centre. These dimensions, together with the four symmetrical waterways gave a facial area too small for profilometer measurements to be made. To circumvent this problem, the following procedure was tried. Abrading of the counterface with silicon carbide papers was chosen as a means of surface preparation rather than mechanical grinding since grinding requires that each surface be checked with a profilometer as no particular surface finish can be guaranteed for any set of grinding conditions. It was hoped that abrading the counterface with various grades of abrasive paper would give reproduceible surface finishes. To this end, a chuck was made to hold the counterface in position over a rotating metallographic polishing wheel with a given grade of abrasive paper adhered to the wheel. It was intended that the roughness of the prepared counterface be found by abrading a 'blank' of identical material (under the same conditions) with a surface area large enough to allow profilometer readings to be taken. However, it was found that this technique gave the blank finishes with very poor reproducibility and so the surface roughness of the actual counterfaces could not be reliably predicted. The original counterface design was therefore scrapped in

favour of the larger model which allows direct roughness measurement and therefore allows mechanical grinding to be used as a means of surface preparation.

The only problem to arise with the new geometry was that the leading edges of the four waterways (slots cut through the wall of the hollow' bits') tended to act as cutting tools, planing away the polymer specimens rather than allowing the relative sliding of the specimen and counterface surfaces. To prevent this undesirable effect, the sharp (90°) edges of the slots were broken and finely rounded off with a fine grade dressing stick.

3.8 REPRODUCIBILITY OF RESULTS

The reproducibility of results from any experimental system depends upon the degree of control over the operating variables which affect the results. Implementation of a standard testing procedure can be used to evaluate the reproducibility of a testing system and show whether results are meaningful.

In this regard, a series of preliminary tests, using the final test geometry, were conducted under supposedly identical conditions of load, speed, counterface roughness and lubricant type. Each test was divided into half hour intervals to allow the weight-loss measurements to be carried out. The weight losses were converted into volume losses and the cumulative volume losses plotted against sliding distance. A straight line was fitted to the points by means of regression and correlation coefficients obtained were typically greater than 0.99. The slopes of the volume loss versus sliding distance plots were taken to be the steady-state wear rates for each test. Table 3.6 summarises the results of these reproducibility tests.

TABLE 3.5. : Reproducibility of test results

TEST	R_a(μm)	PRESSURE (MPa)	VELOCITY (m/s)	LUBRICANT	WEAR RATE (mm^3/m)	MATERIAL
1	1.05	1	0.13	water	3.069 E-2	UHMWPE
2	1.07	1	0.13	water	3.390 E-2	UHMWPE
3	1.09	1	0.13	water	3.540 E-2	UHMWPE
Average	1.07				3.333 E-2	
%deviation	2				7.23	

Considering the viscoelastic properties of the material, the interrupted test procedure used and the relatively small weight losses measured, the reproducibility of the test was considered to be acceptable under these conditions. Perhaps the largest influence on reproducibility here is the counterface roughness, which cannot be reproduced easily and has a marked effect on the wear rate of the material.

3.9 SCANNING ELECTRON MICROSCOPY (SEM)

After the completion of each test, both the counterface and the polymer specimen were examined under the SEM. The polymer discs were mounted on aluminium stubs with cyanoacrylate adhesive and ELECTRODAG 915 conductive paint was applied to the sides to form a conducting path between polymer and stub.

Finally, a POLARON E5100 unit was used to apply a conductive Au/Pd coating to the polymer. The used counterfaces were also Au/Pd coated to preserve any transferred material from being damaged by the electron beam. After examination in the CAMBRIDGE S-200 SEM, the polymer discs were stored and the counterfaces reground for the next series of tests.

3.10 MATERIALS

Table 3.6 is a list of the materials tested which shows the abbreviations used in naming the polymers along with their trade names [37,65].

TABLE 3.6 : A list of the materials tests

ABBREVIATION	GENERIC NAME OF POLYMER	TRADE NAME
UHMWPE	ultra high molecular weight polyethylene	SOLIDUR 10100
UHMWPE/FILL	ultra high molecular weight polyethylene with an organic friction-reducing filler	SOLIDUR DS
POM	polyoxymethylene (polyacetal)	DELRIN 500
PETP	poly(ethylene terephthalate) (a semi-crystalline thermoplastic polyester)	ERTALYTE
PA6/MoS_2	polyamide 6 (nylon 6) with molybdenum disulphide filler	NYALTRON GSM
P(A-I)/GR	poly(amide-imide) copolymer with 12% graphite filler and 3% PTFE	TORLON 4301

To assist in the interpretation of wear data, the materials were characterised by means of standard mechanical tests and by observation of their sections using transmitted light.

3.10.1 Optical Microscopy

The materials were sectioned into 5 micrometre thick slices with an ANGLIA SCIENTIFIC 200 sledge microtome. The polyester and poly(amide-imide) specimens were too brittle to be thin-sectioned by this technique as they displayed a tendency to crumble or 'powder'. The slices of material were mounted on ground glass slides with coverslips using Canada balsam as a fixative and observed using transmitted light with a NIKON OPTIPHOT-POL polarising light microscope.

Figure 3.7(a), (b) and (c) show the structures of UHMWPE/FILL, POM and PA6/MoS_2 respectively.

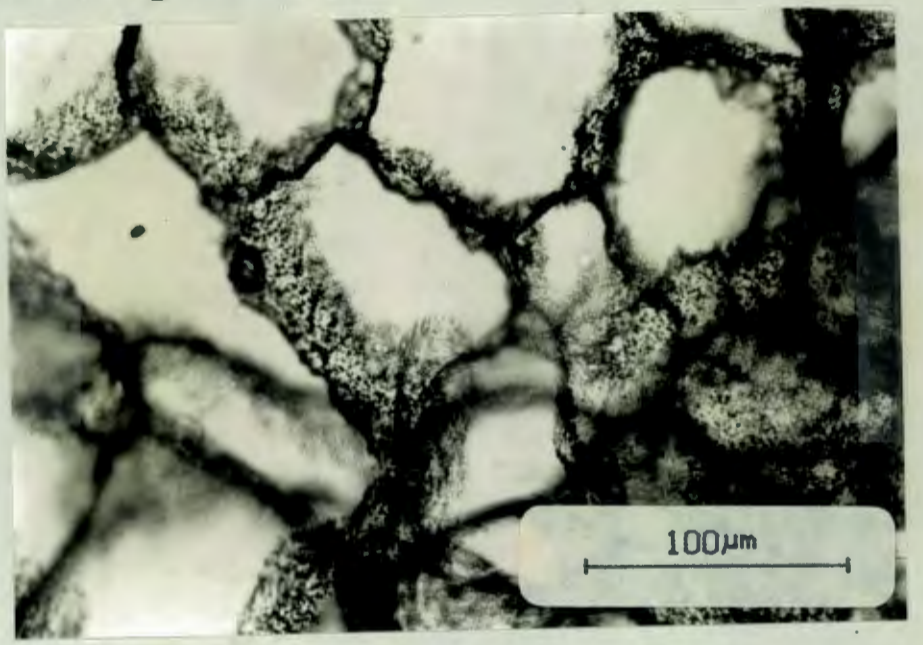

FIGURE 3.7(a) : UHMWPE/FILL section showing the particulate structure of this material, achieved by a process of sintering the mixture of powdered polyethylene and an additive. It is uncertain if the darker, mottled areas at particle boundaries are associated with the filler.

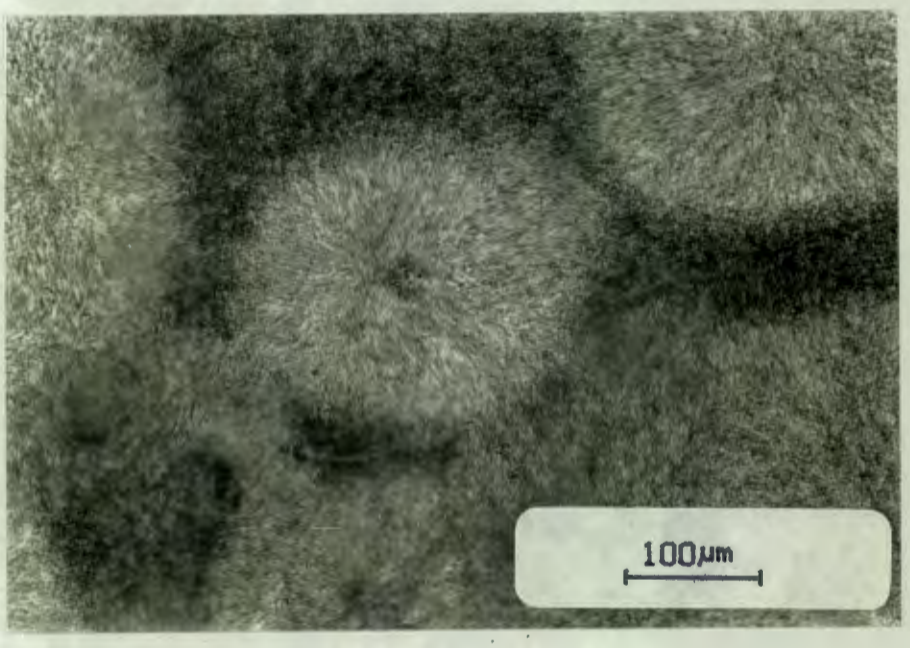

FIGURE 3.7(b) : POM section showing the spherulitic structure of this extruded material (crossed polars).

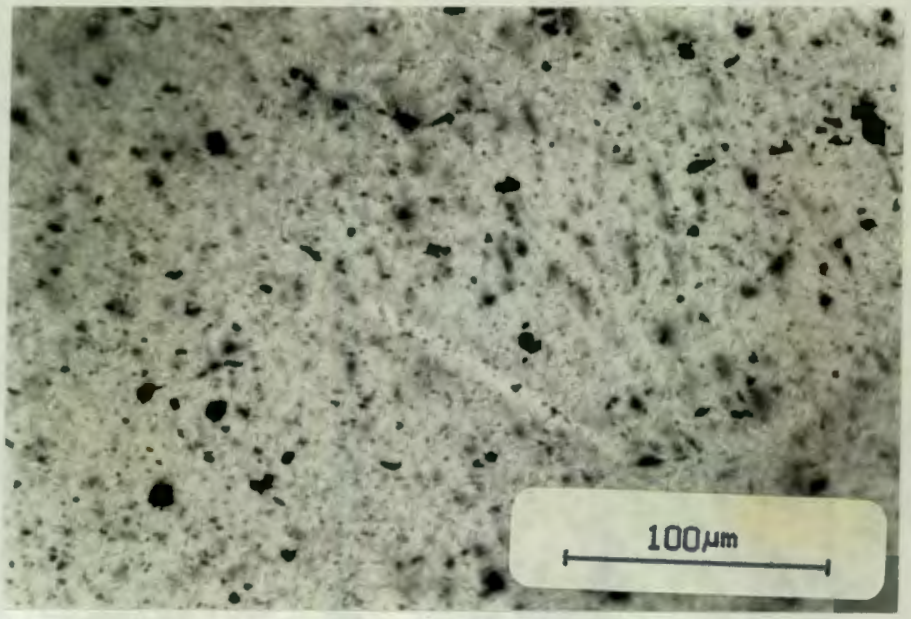

FIGURE 3.7(c) : PA6/MoS_2 section showing the molybdenum disulphide filler particles which appear as black specks.

3.10.2 Mechanical Tests

Tensile, impact and Shore 'D' hardness tests were performed on the materials according to ASTM D638, D256 and D2240 standards respectively. The results of these tests appear in Table 3.7 along with some other materials properties taken from literature [37,65]. The laboratory tests have a reproducibility of ± 5%.

The fracture surfaces of the specimens from the tensile tests were examined under the scanning electron microscope in an attempt to correlate their appearance with the tensile data obtained. Typical examples of these fracture surfaces are shown in figs. 3.8(a)-(g).

TABLE 3.7 : Materials properties. Note: an * indicates that the value concerned is taken from literature.

POLYMER	UHMWPE	UMPWPE/FILL	POM	PETP	PA6/MoS_2	P(A-I)/GR
UTS (N/mm^2)	29	27	78	78	58	83
FRACTURE STRESS (N/mm^2)	60	63	83	217	135	87
% ELONGATION	290	320	38	34	69	5
ELASTIC MODULUS (N/mm^2)	232	220	927	1049	743	2230
SHORE "D" HARDNESS	66	64	81	86	75	91
IZOD IMPACT TOUGHNESS (J/m)	NO BREAK	NO BREAK	55	29	-	32
DENSITY (g/cm^3)	0.94	0.96	1.42	1.38	1.16	1.45
MELTING TEMPERATURE (°C) *	137	137	175	255	220	260
THERMAL CONDUCTIVITY (W/°C/m) *	0.42	-	0.37	0.29	0.36	0.54

The SEM micrographs of the fracture surfaces appear below.

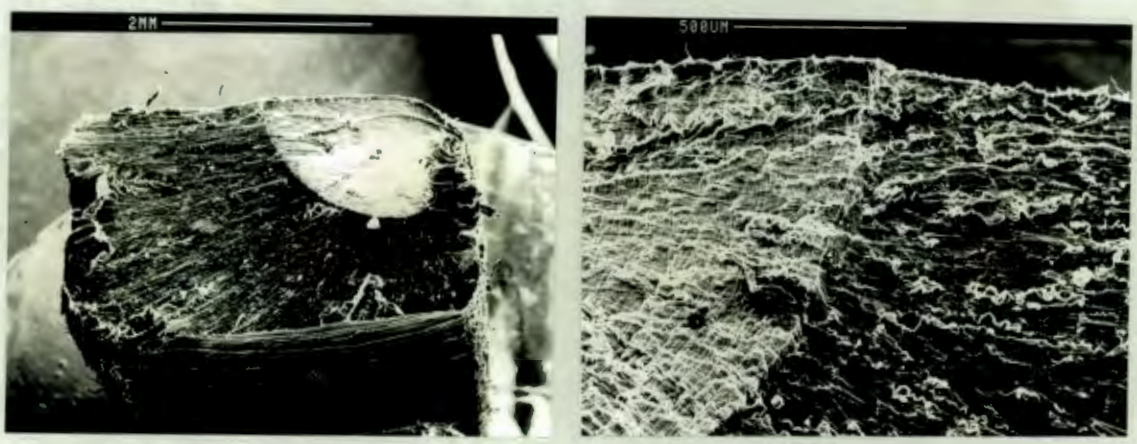

FIGURE 3.8(a) and (b) : Two magnifications of the fracture surface typical of UHMWPE, UHMWPE/FILL and PA6/MoS_2.

The UHMWPE, UHMWPE/FILL and PA6/MoS_2 surfaces typically show two distinct areas (fig. 3.8(a) and (b)). The first is the lighter area of transverse curved boundaries or striations (crazing) which forms because of the pulling up, separation and collapsing of walls as the crack propagates in what is essentially a ductile tear fracture. This is in clear contrast to the residual stress fracture area, which has lines radiating outward in the direction of crack propagation and parallel to this direction. In the case of POM, the fracture area shows peaks and fibrils radiating from the centre of the specimen (fig. 3.8(c)). Figure 3.8(d) is a clear view of the individual fibrils. The microporosity of the material is due to the manufacturing process and is caused by the transition from low to high density during crystallisation [31].

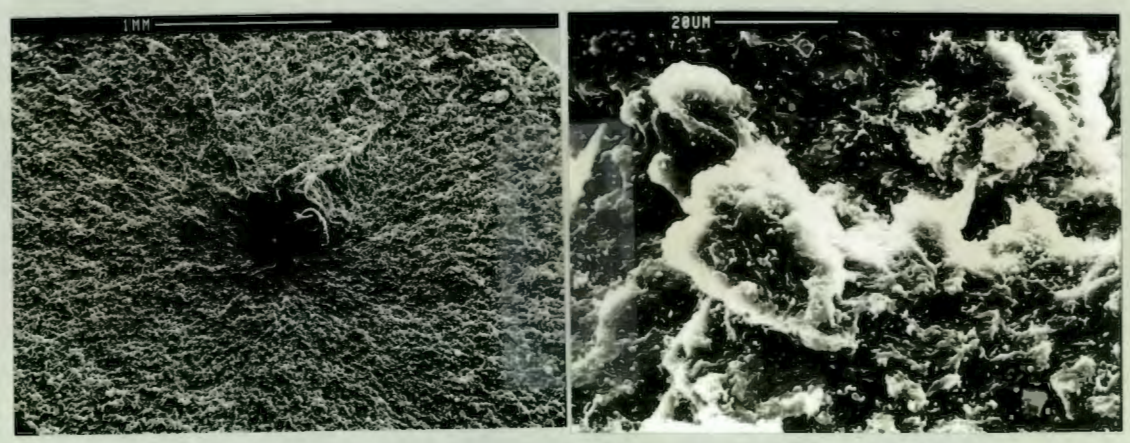

FIGURE 3.8(c) and (d) : POM fracture surface.

Figure 3.8(e) shows the extreme necking which PETP displayed while figs. 3.8(f) and (g) show the fracture surface of the brittle P(A-I)/GR.

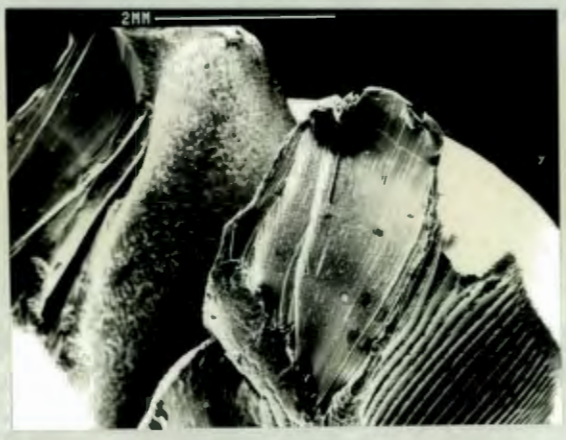

FIGURE 3.8(e) : Necking of the PETP specimen.

FIGURE 3.8(f) and (g) : P(A-I)/GR fracture surface showing debonding and fracture of graphite particles.

CHAPTER 4

RESULTS AND DISCUSSION

4.1 INTRODUCTION

This chapter deals with the results of the matrix of experimental tests which were conducted under various combinations of applied load, sliding velocity and counterface roughness.

In order to establish the effect of an increase in counterface roughness, tests were conducted mainly at two different values of R_a roughness, namely 0.25 micrometres and 1 micrometre. These were done for different pressures and over a wide range of velocities. In addition, some tests were carried out at an R_a of 0.6 micrometres for selected conditions of pressure and velocity, in order to check the relationship between wear rate and counterface roughness.

The effect of applied load or "bearing" pressure was monitored by carrying out tests mainly at two different pressures, namely 1 MPa and 5 MPa. This was done for different conditions of counterface roughness and over a wide range of velocities. In addition, some tests were done at a pressure of 3 MPa for selected conditions of counterface roughness and sliding velocity, in order to check the relationship between wear rate and pressure.

To investigate the effect of sliding velocity, tests were conducted at five different values of velocity (encompassing the full range of the experimental rig's capabilities from 0.13 m/s to 2.268 m/s, a seventeen fold increase) under various permutations of pressure and counterface roughness.

For all of the test conditions the lubricating medium was tapwater.

Table 4.1 summarises the matrix of tests completed.

TABLE 4.1 : The testing matrix. An "X" indicates that testing under such conditions was completed for all the materials.

Series A : Counterface R_a = 1 ± 0.1 micrometres

		V(m/s)				
		0.130	0.616	1.063	1.815	2.268
P(MPa)	1	X	X	X	X	X
	3	X				
	5	X	X	X	X	X

Series B : Counterface R_a = 0.25 ± 0.03 micrometres

		V(m/s)				
		0.130	0.616	1.063	1.815	2.268
P(MPa)	1	X	X	X	X	X
	5	X	X	X	X	X

Series C : Counterface R_a = 0.60 ± 0.01 micrometres

		V(m/s)
		0.130
P(MPa)	5	X

4.2 THE EFFECT OF COUNTERFACE ROUGHNESS

4.2.1 General Trends and Comparisons

It is generally recognised that the rate of wear of a polymeric material in relative sliding contact with a steel counterface will be affected by the topography of that counterface. As mentioned in Chapter 2, there are various ways of characterising such a topography, and in this case the R_a or centre line average (c.l.a.) value was used mainly because it is quick and easy to monitor with relatively simple equipment and because other researchers have used this parameter [27,60,61,28,50,62] as a means of characterisation.

Fig. 4.1 shows the wear rates found for the six materials at three values of counterface roughness. The error associated with these values is typically up to twenty percent and this is thought to be due mainly to the error associated with reproducing a given counterface roughness value, which varies by up to fifteen percent.

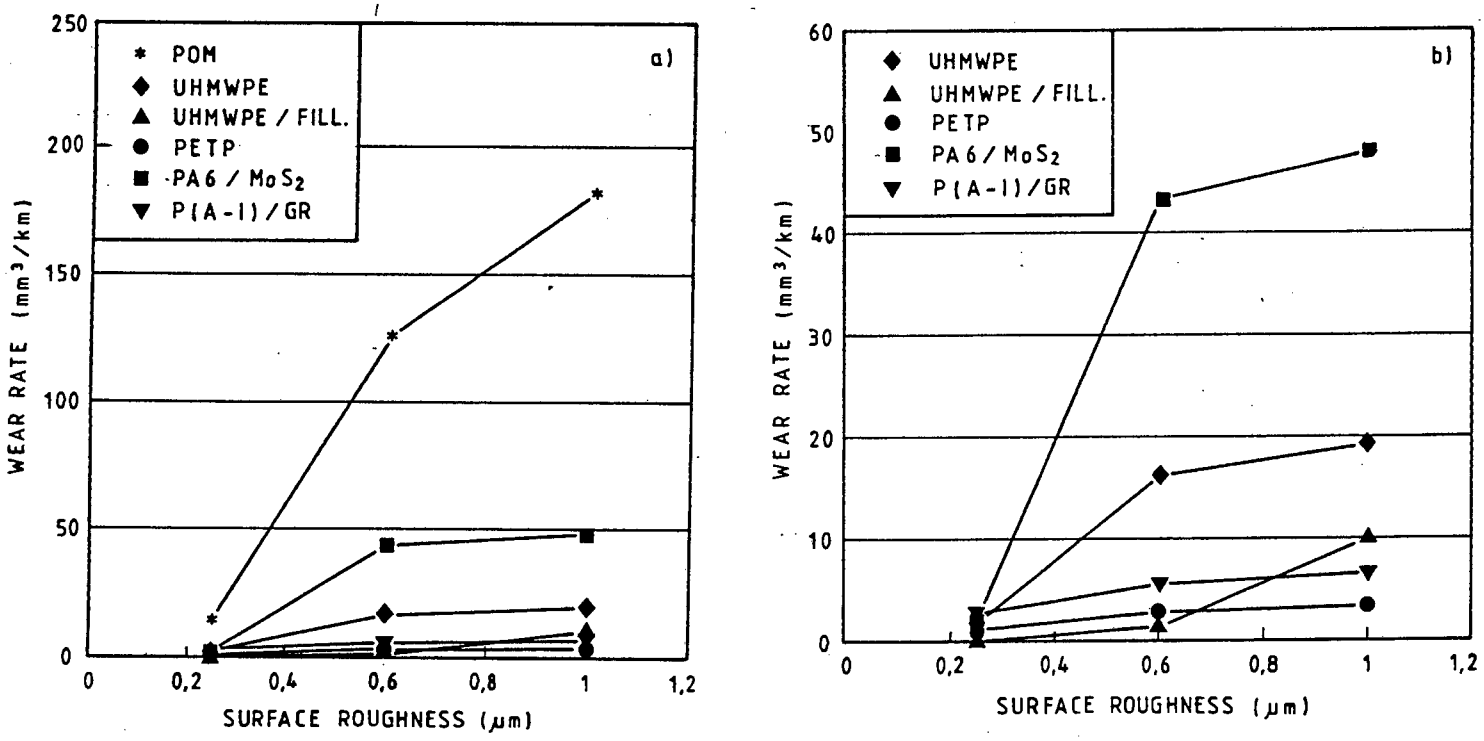

FIGURE 4.1(a) & (b) : Wear rate vs counterface roughness for all the test materials at 0.13 m/s and 5 MPa. Note that the lines connecting points are to help identify association of points and are not intended to suggest that a straight line relationship exists between points.

All the materials with the exception of filled UHMWPE (which will be discussed later) appear to follow a similar trend. All the materials exhibit an increase in steady state wear rate if the counterface roughness is increased. However, the relationship does not appear to be linear but rather rapidly increasing in the lower regions of roughness and less rapidly increasing in the higher regions of roughness.

Plotting the data in a log-linear fashion with wear rate values on the logarithmic axis serves only to accentuate the change in gradient. A log-log plot yields a similar picture to that obtained in the original linear-linear plot of fig. 4.1. The log-linear and log-log plots can be seen in fig. 4.2.

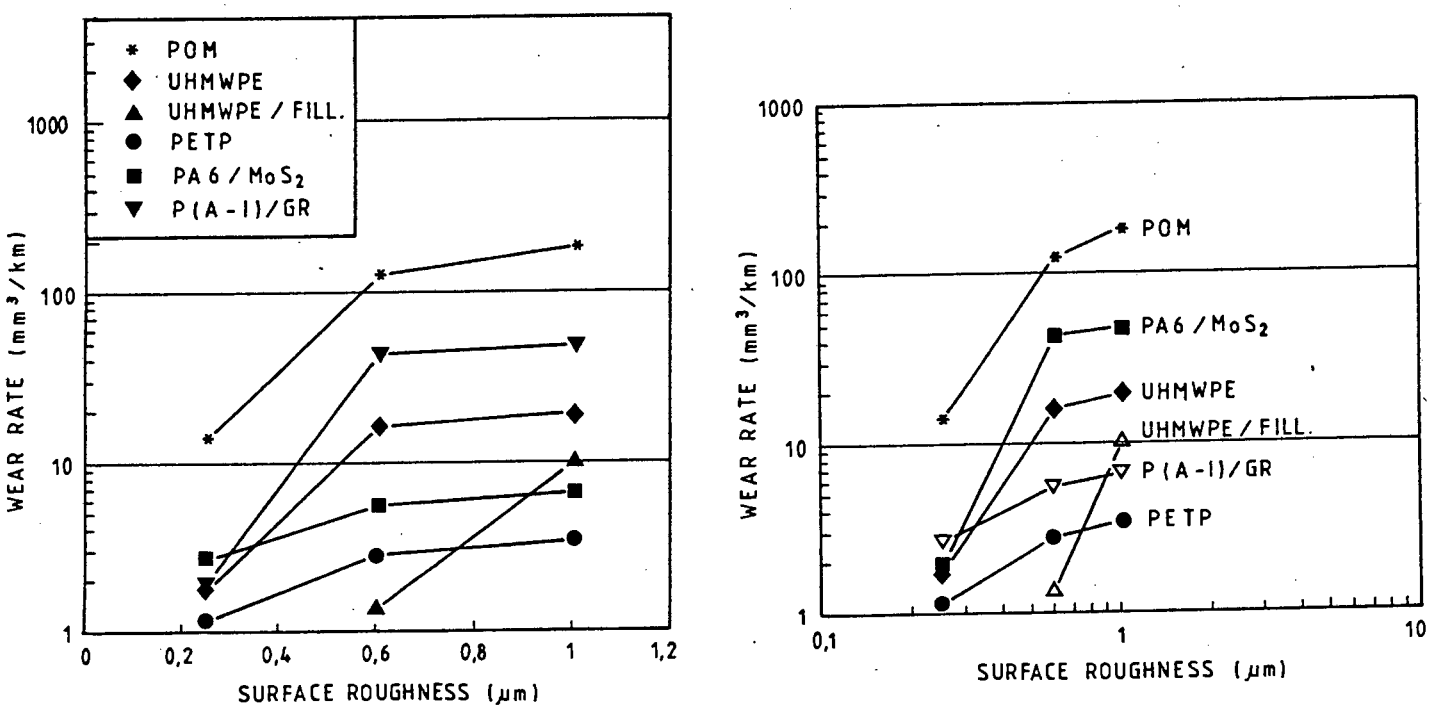

FIGURE 4.2 : Wear rate vs counterface roughness on log-linear and log-log scales respectively. Note: The result for UHMWPE/FILL at 0.2 micrometres does not appear because the wear rate was found to be effectively zero.

Lloyd [42], working with water lubricated UHMWPE sliding against hardened AISI 431 steel at 0.25 m/s under 10 MPa, investigated the effect of counterface roughness on wear rate in pin on plate, reciprocating conditions. The R_a value was varied between 0.1 micrometres and 1 micrometre and the specific wear rate, when plotted out against the counterface roughness in a log-linear fashion showed some scatter but a straight line was fitted to the data, giving the relationship as :

Specific Wear Rate (mm^3/Nm) = $1.096 \times 10^{-8} e^{(7.67\ c.l.a.)}$

The data shown in fig. 4.1 do not appear to conform to this type of relationship (see fig. 4.3(a)).

Dowson et al [28], using a pin on plate reciprocating test of UHMWPE on EN58J steel at 0.25 m/s under pressures of between 6 and 14 MPa with water lubrication found a straight line relationship when results were plotted on a log-log scale. This relationship was quoted as :

$k(mm^3/Nm) = 4.0 \times 10^{-5} (R_a)^{1.2}$

The data shown in fig. 4.1 do not fit this relationship (see fig. 4.3(b)).

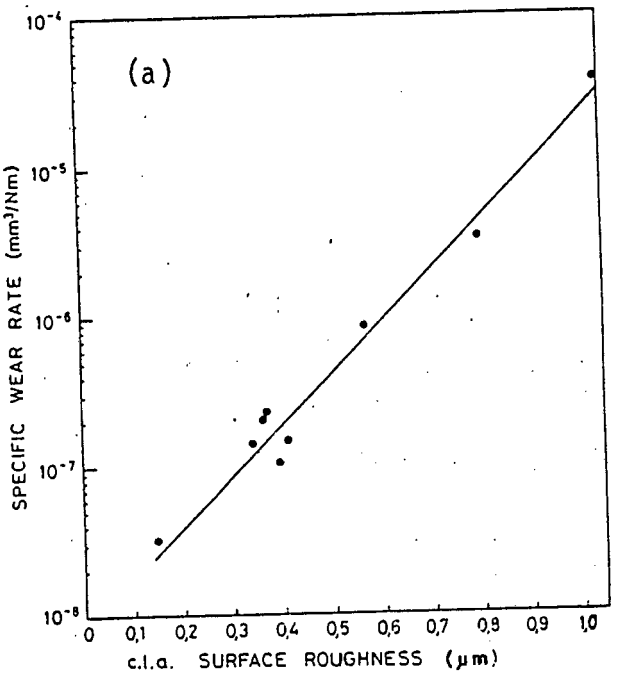

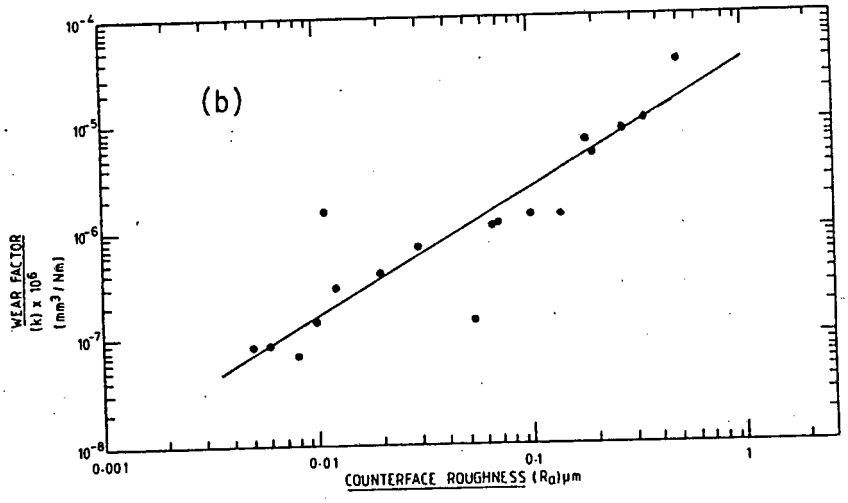

FIGURE 4.3(a) & (b) : Wear vs counterface roughness relationships after Lloyd [42] and Dowson [28] respectively.

4.2.2. Proposed Wear Model

It appears therefore that the author's wear rate versus counterface roughness results do not show a linear relationship on a linear-linear scale, a log-linear scale (as in the case of Lloyd [42]) or a log-log scale (as in the case of Dowson et al [28]). A rough model, using the data for UHMWPE as an example, is proposed in fig. 4.4.

This shows a transition in gradient from rapidly increasing at lower counterface roughness to more gradually increasing at higher counterface roughness. There is a definite change in gradient between R_a values of 0.25 and 0.6 micrometres, with the point of inflexion probably between 0.25 and 0.4 micrometres.

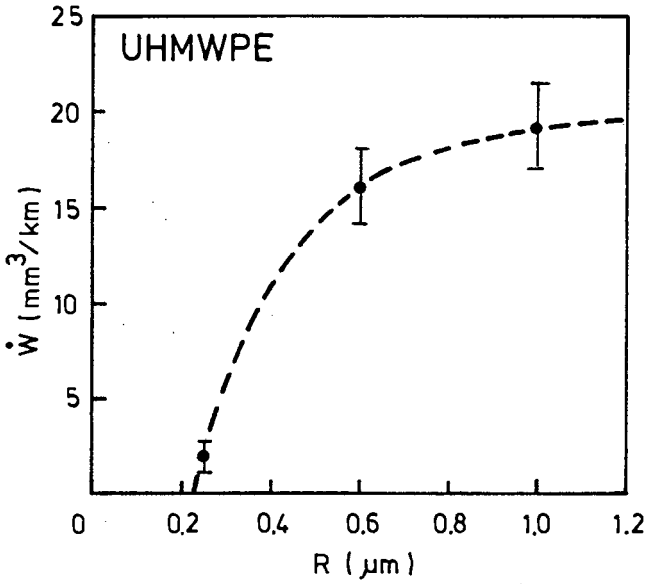

FIGURE 4.4 : Proposed model of the effect of counterface roughness on steady state wear rate.

Tanaka and Nagai [60] have used a pin on disk unidirectional test with LDPE and HDPE sliding against NAK55 steel. The counterface preparation technique gave surfaces ranging from 0.025 to 1.3 micrometres R_a, with a random texture or lay. The dry sliding tests were conducted at 0.01 m/s under approximately 1 MPa to prevent surface melting. The wear rate versus roughness results were plotted on a linear-linear scale and are shown in fig. 2.6(a) and (b) in Chapter 2. It is clear that the relationship proposed by Tanaka and Nagai is in close agreement with the model suggested by this author.

Czichos [21] has found a similar relationship between wear rate and counterface roughness, with the wear rate of PA6 shown to be weakly dependent on roughness above an R_z value of 0.6 micrometres.

It is possible that there are more similarities between the author's work and that of Tanaka and Nagai or Czichos than between the author's work and that of Lloyd or Dowson et al. For instance, Lloyd and Dowson both use a water lubricated reciprocating test with the sliding direction always at right angles to the lay of the counterface. Tanaka and Nagai use a dry, low speed, low pressure, unidirectional test with sliding across a counterface with no directionality in its lay, that is, a randomly oriented lay. The author has used a water lubricated, unidirectional test with effectively a randomly oriented counterface (since any point on the polymer surface sees a constantly changing counterface orientation). It is probable that the dry test approach of Tanaka and Nagai is similar to the water lubricated approach of the author since in the dry case, the low speeds and low pressures used prevented appreciable surface melting while in the wet case it is likely that the water performs essentially a cooling effect only, as water has poor lubricity under boundary lubrication conditions. These relationships are presented schematically in Table 4.2.

TABLE 4.2 : Comparison of test methods

Lloyd [42] / Dowson [28]	RECIPROCATING	WET	SLIDING AT 90° TO COUNTERFACE LAY
Author	UNIDIRECTIONAL	WET	SLIDING ACROSS RANDOM LAY
Tanaka [60]	UNIDIRECTIONAL	DRY	SLIDING ACROSS RANDOM LAY

The shape of the curve in figs. 2.6 (a) and (b) is determined by the interaction of mechanisms. It may be reasonable to assume that the predominant wear mechanism is different between the two regions. Wear in the gradually increasing range may be assumed to be due to fatigue originating from tensile stresses and partially due to transfer. Wear in the rapidly increasing range may occur due to an abrasive action of counterface asperities as well as due to transfer [60].

Consider now the author's results. The shape of the curve in the model shown in fig. 4.4 is probably due to an interaction or change in wear mechanism as the R_a of the counterface changes.

At lower values of R_a (the steep part of the curve) it is most likely that wear of the polymer is due to a process of film transfer. This transfer to a fairly smooth counterface is initiated by adhesive interactions at the junctions between the polymer surface and the counterface asperities, leading to the displacement of relatively small sheets or particles of polymer onto the steel surface. The sliding action causes these polymer fragments to accumulate preferentially in the valleys between the counterface asperities, where the adhered transfer is least likely to be disturbed. The coalescence of transfer debris from repeated adhesive interactions results in the formation of a fairly coherent transfer film throughout the valleys of the counterface. The existence of a few relatively large asperities may deform the polymer surface on a larger scale than the adhesive interactions (by cutting and ploughing if they are sharp or by rucking up the surface into wave-like patterns if they are rounded). Fig. 4.5 (a) shows the appearance of a typical counterface from the 0.25 micrometre tests and fig. 4.5(b) the accompanying polymer surface.

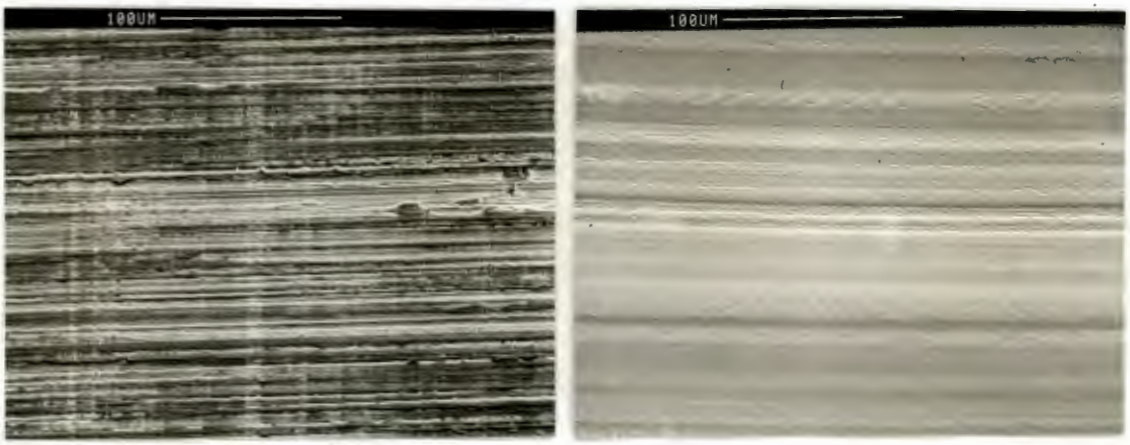

FIGURE 4.5(a) & (b) : Typical views of counterface and polymer respectively. R_a = 0.25 micrometres, the material is UHMWPE. Sliding is from bottom to top in (a) and from right to left in (b).

The counterface shows extensive valley transfer with polymer adhering to the sides of machining ridges, while the surface of the polymer specimen displays broad, shallow bands. The surfaces of the bands are either fairly smooth or display a mottled or wavy appearance. This seems to support the argument of an adhesive/fatigue mechanism dominating at lower counterface roughnesses.

At the highest value of counterface roughness, it is likely that a slightly different mechanism is in operation, with the larger asperities now having a more aggresive or disruptive effect on the polymer surface. Severe rucking up of the surface into bumpy, wave-like patterns will occur, while some cutting by sharper asperities may take place. Fig. 4.6(a) and (b) show typical views of the specimen and counterface from the 1 micrometre tests.

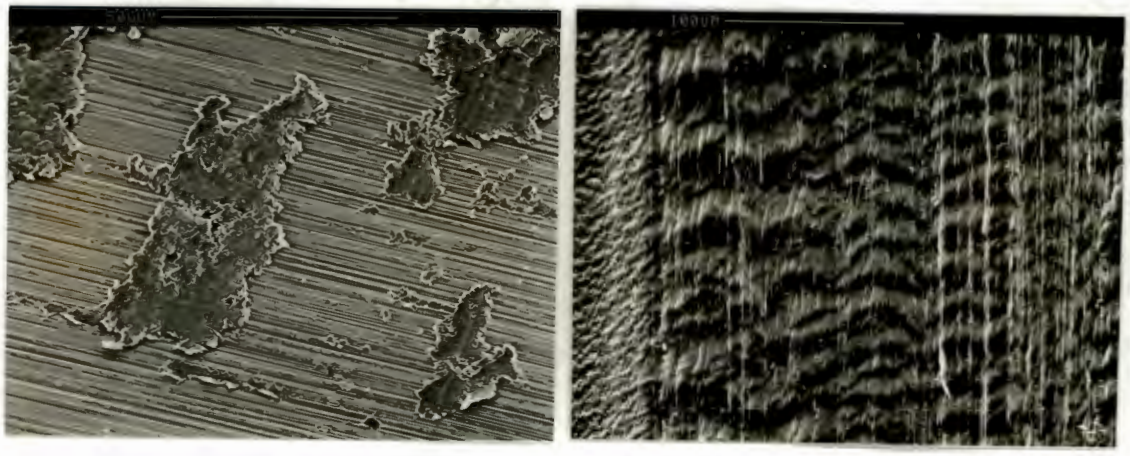

FIGURE 4.6(a) & (b) : The counterface and polymer specimen surfaces respectively. R_a = 1 micrometre, the material is UHMWPE. Sliding is from top right to bottom left in (a) and from top to bottom in (b).

It is evident from fig. 4.6(b) that severe deformation of the polymer surface has occurred, with larger asperities having caused broad wave-like bands perpendicular to the sliding direction. Some scratches and tears parallel to the sliding direction are also evident, probably as a result of interactions with sharper asperities. From consideration of fig. 4.6(a) it appears that transfer has occurred in the form of large, poorly adhered sheets, with little or no transfer of the type found at lower R_a values.

It is considered that wear at the higher values of counterface roughness proceeds by a mechanism of fatigue/abrasion. The large asperities pull the surface of the polymer up into large wave-like shapes by a process of repeated deformation until large sheets of polymer become dislodged and are draped or weakly adhered across the steel surface. The sheets may coalesce on the steel surface to form larger sheets or the fairly weak bond between polymer and steel may be broken and the sheet readheres to the polymer surface in a process of "back" transfer. The sharper asperities on the steel counterface cause material removal from the polymer surface by a process of cutting or tearing. Fig. 4.7 shows a polymer surface which has been subjected to cutting and back transfer.

FIGURE 4.7 : UHMWPE surface showing cutting and back transfer. R_a = 1 micrometre, sliding is from top right to bottom left.

The thin groove which is evident across the polymer surface is a result of cutting by a sharp asperity, while the fragment near the centre of the photograph is the result of back transfer. For purposes of comparison, it may be useful to consider comments made by Tanaka and Nagai on their work. They comment that in the case of very rough counterfaces, SEM examination indicated that a number of thick and large lumps were transferred, while many scratches remained which were not filled with polymer. When the counterface roughness decreases, the transfer of thick and large lumps also decreases [60]. Czichos, when discussing his plots of wear rate versus counterface roughness, makes the following comment : ".... wear behaviour in the left-hand region of the diagram is governed mainly by adhesive processes, i.e. formation and rupture of adhesively bonded material parts, whereas for counterface roughness values higher than those related to minimum wear, abrasive processes are the dominating mechanisms" [21].

Examination of the sliding surfaces from the 0.6 micrometres R_a tests reveals an appearance between that of the surfaces from the 0.25 and 1 micrometre tests, but closer in appearance to the 1 micrometre test surfaces. This is to be expected from consideration of the wear rates and mechanisms operating in each case. Figs. 4.8(a) and (b) show an example of the sliding surfaces from the 0.6 micrometre tests.

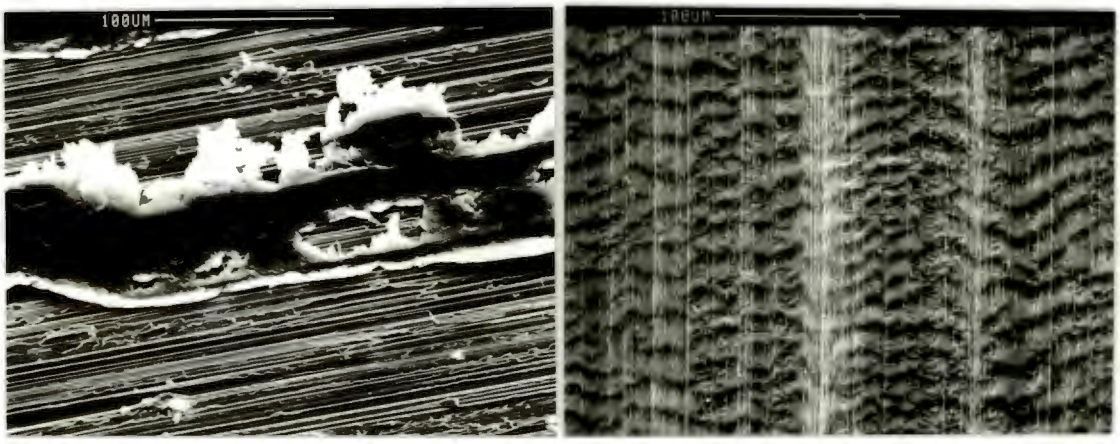

FIGURE 4.8(a) & (b) : An example of the counterface and polymer specimen surfaces respectively, from the 0.6 micrometre tests. The material is UHMWPE and the sliding direction is from top to bottom in both cases.

The counterface in fig. 4.8(a) shows the existence of large transfer sheets, similar in appearance to, but smaller in size than those from 1 micrometre surfaces. It is also evident that a very small amount of the smaller scale, coherent valley transfer is present. There is therefore a mixed mode of transfer present, closer in appearance to the transfer on 1 micrometre surfaces but retaining similarities to that found on 0.25 micrometre surfaces. The polymer specimen surfaces are covered with wave-like patterns, transverse to the sliding direction suggesting a fairly severe fatigue action of counterface asperities. However, no relatively smooth surfaces (as for 0.25 micrometre test surfaces) or appreciably cut up or abraded surfaces (as sometimes occur for 1 micrometre test surfaces) seem to appear.

The reason that the curve of wear rate versus counterface roughness tends towards a decreasing slope (flattening out) as the roughness increases, can probably be explained in terms of the mechanism which becomes more dominant as the R_a value increases. For a situation in which abrasion or fatigue by counterface asperities dominates, a point will be reached where enlarging counterface asperities further (increasing the R_a value) will not yield directly proportionate increases in wear volume of the polymer specimen.

This is because increasing the size of each asperity will tend to decrease the number of contacts for a given nominal contact area A_o. Thus for a given A_o, increasing roughness will yield fewer contacts and the real contact area A_r will show smaller and smaller increases. This in fact seems to suggest that a point will be reached where wear volume will (short of gross melting) become independent of counterface roughness since there exists a maximum size "chunk" of material which can be removed at each interaction.

4.2.3 Deviations from and Modifications to the Model

A model for the proposed mechanism of polymer wear with increasing counterface roughness has been presented and discussed in general terms. All the micrographs shown in support of this model have been of surfaces of, or associated with, a material which shows "typical" behaviour, notably UHMWPE. It should be stressed that not all the wear surfaces examined showed an identical appearance to those from the UHMWPE tests. This is probably because modifications to the basic mechanistic model of wear are necessary due to the differing mechanical properties of the six materials tested. The responses of the individual materials to increasing counterface roughness will obviously differ slightly according to the individual mechanical properties. These modifications to, or deviations from the model should be mentioned.

Materials with a higher Shore "D" hardness value (see Table 3.7) would appear to have a more brittle response to the movement of counterface asperities. Softer materials like UHMWPE flow more easily under the action of the steel asperities and can be more easily pulled up into the wavy striations associated with the fatigue wear process. Thus, these "fatigue striations" should be abundant on the wear surface and should be fairly prominent or well developed because of the material's ability to absorb large amounts of deformation through successive straining, without breaking (compare % elongation values in Table 3.7).

Furthermore, material loss in these softer materials, due to abrasive cutting or chipping, should be low. This is due to the ease with which hard asperities cause ploughing of the polymer surface and material pile-up alongside wear grooves with little actual volume loss. That is, the surface can be plastically rearranged without the material being chipped or cut away. It is likely then that most of the wear grooves displayed in softer materials should be smooth in profile, possibly with fatigue patterns running across the base of the grooves, while only a small proportion of grooves should show a jagged appearance, where material has been torn from the surface. SEM observations of the softer surfaces seem to confirm the above statements. A typical example is shown in fig. 4.9.

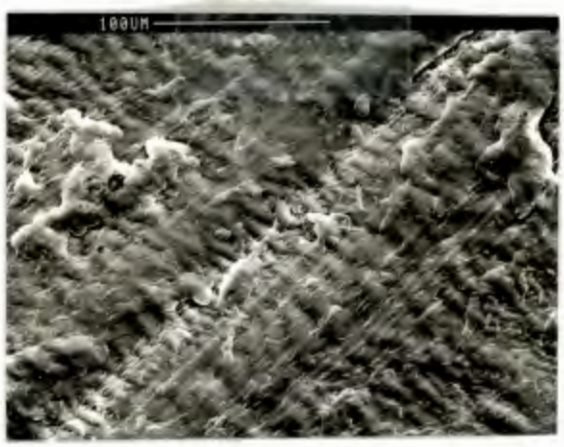

FIGURE 4.9 : Shallow groove in an UHMWPE/FILL surface showing smooth edges and wave-like features both in the groove and across the rest of the surface. R_a of counterface is 1 micrometre, sliding direction is from top right to bottom left.

SEM observations of the harder surfaces indicate shallower striations on the polymer and the presence of wear grooves with more jagged edges. An example can be seen in fig. 4.10.

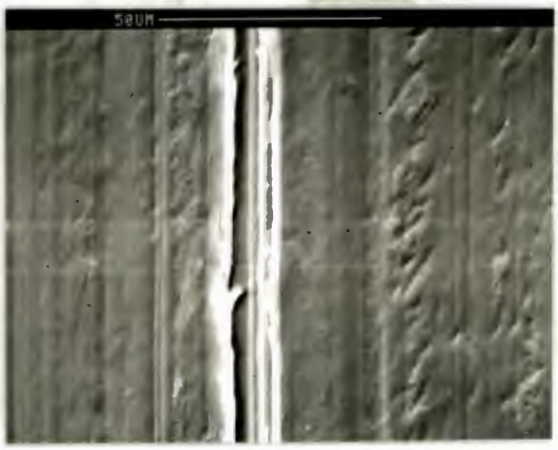

FIGURE 4.10 : PETP surface showing shallower striations and wear grooves with more jagged edges. R_a of counterface is 1 micrometre, sliding direction is from bottom to top.

When considering the behaviour of the individual materials, there are certain questions which should be addressed, namely :

1. Why does UHMWPE/FILL show a different response from the other polymers to an increase in counterface roughness (see fig. 4.1(b) ?

2. Why do PETP and P(A-I)/GR in particular show less sensitivity to changes in counterface roughness ?

3. Why is POM consistently a poor performer ?

4.2.3.1 UHMWPE/FILL

UHMWPE/FILL has considerably lower wear rates than the other polymers at 0.25 and 0.6 micrometres, while at 1 micrometre its wear rate becomes greater than that of some of the other polymers. This gives the wear rate versus counterface roughness curve an increasing gradient up to 1 micrometre unlike the curves for the other materials, which all have decreasing gradients. This behaviour seems to be explained through SEM observations of the counterface. The general wear model proposes that extensive valley transfer occurs at 0.25 micrometres but that an increase in roughness to 0.6 micrometres causes a change in transfer

characteristics from valley transfer to larger, poorly adhered sheets. With UHMWPE/FILL however, a thick, coherent valley transfer film was observed even at 0.6 micrometres, with the alternative mode of transfer visible only at 1 micrometre. This transfer at 0.6 micrometres is shown in fig. 4.11.

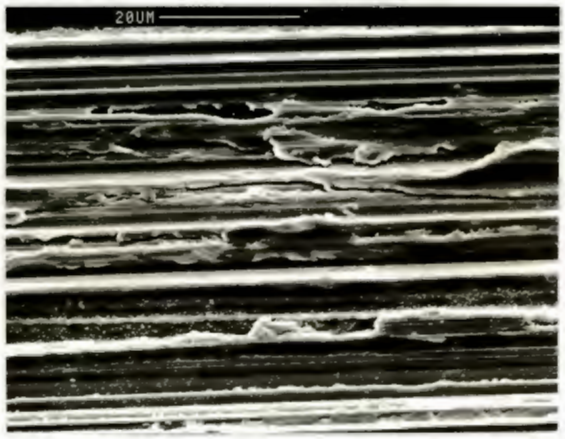

FIGURE 4.11 : Valley transfer film on the UHMWPE/FILL counterface from a 0.6 micrometre R_a test. Sliding is from top to bottom.

The change in wear mechanism therefore occurs at higher counterface roughnesses than for the model based on UHMWPE because UHMWPE/FILL is able to form coherent valley transfer films on rougher surfaces more easily than UHMWPE. The shape that this "delayed" response gives to the wear rate versus counterface roughness curve suggests that similar behaviour would be observed for the UHMWPE model if roughnesses less than 0.25 micrometres were tested. Extending the model curve to lower roughnesses might show a shape similar to that observed with UHMWPE/FILL at slightly higher roughnesses.

4.2.3.2 PETP and P(A-I)/GR

PETP (along with P(A-I)/GR) shows a less sensitive response to increases in counterface roughness than the other materials and this is primarily related to its transfer characteristics.

Under the pressure and velocity conditions illustrated in fig. 4.1, PETP shows very low wear rates at all values of counterface roughness, and only a slight increase in wear rate with roughness increases. This is most probably due to its ability to form a blanket of transferred material over almost the entire counterface even at the greater roughness values. This blanket can be seen in fig. 4.12.

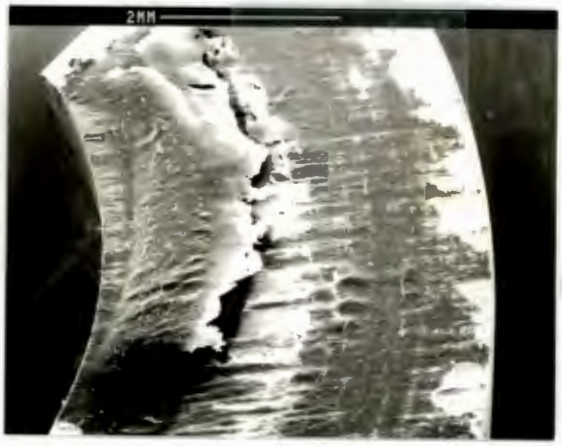

FIGURE 4.12 : The blanket of transfer on the PETP counterface which is seen to be peeling off after being exposed to ultra high vacuum conditions in the photographic preparation process. This is a 1 micrometre counterface and similar transfer films are observed on the 0.6 micrometre counterfaces.

At the lower value of 0.25 micrometres, a coherent valley transfer film exists. PETP thus shows low wear rates at all roughness values because sliding is essentially between two polymer surfaces with little interaction between the metal asperities and the polymer specimen surface.

P(A-I)/GR shows a tendency to polish the counterface down to smaller values of roughness. A profilometer trace of a used counterface that had been cleaned and was relatively free of transfer, showed a drop in roughness from the original 0.22 micrometres value down to 0.09 micrometres. This polishing effect seems most pronounced if the starting value of roughness is already low.

At the higher value of 1 micrometre, no considerable polishing was observed, only the formation of thick lumps of transfer, while at the lower value of 0.25 micrometres polishing and transfer were seen. At the intermediate value of 0.6 micrometres, only slight polishing but extensive transfer were observed. Figs. 4.13 to 4.15 show this behaviour.

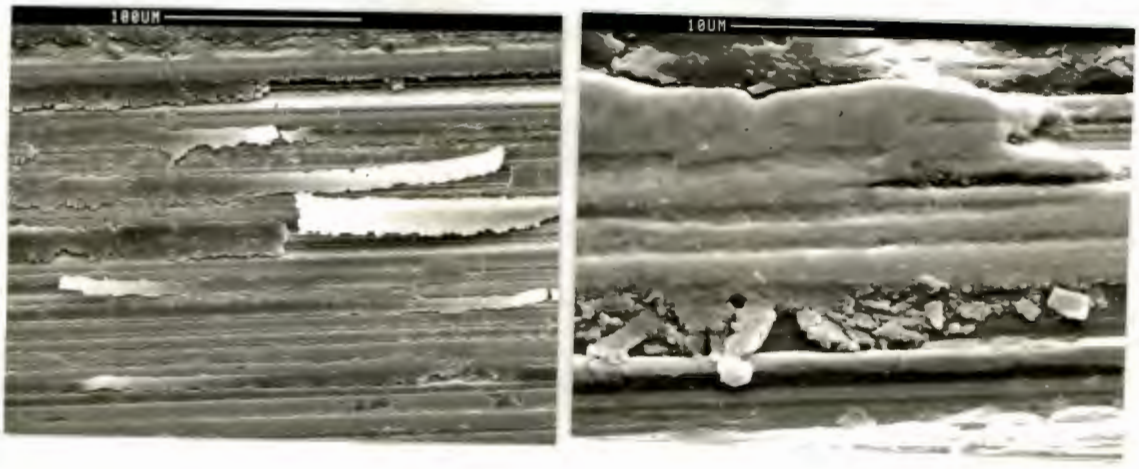

FIGURE 4.13(a) & (b) : Low and high magnifications respectively of the used 1 micrometre P(A-I)/GR counterface showing a thick, lumpy transferred layer. Sliding is from top to bottom in both cases.

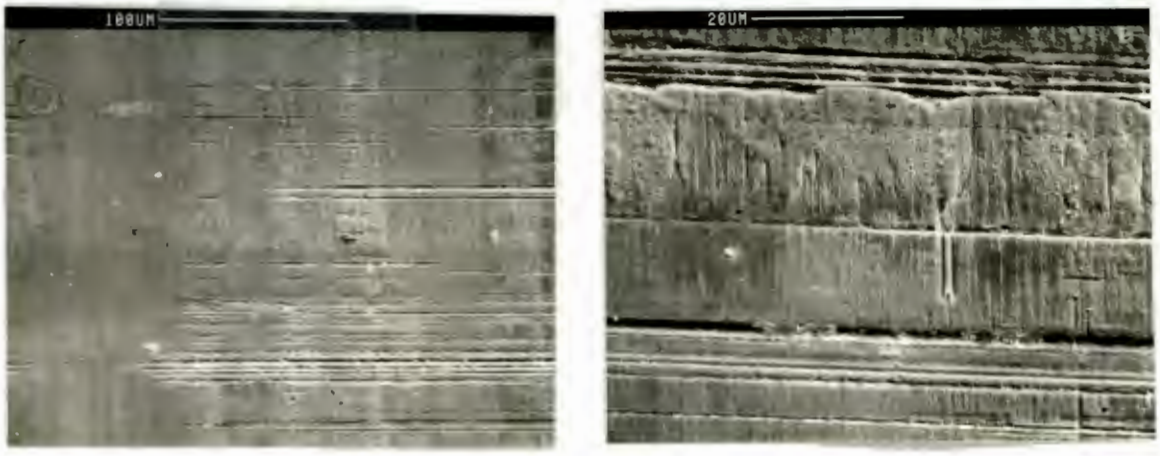

FIGURE 4.14(a) & (b) : Low and high magnifications respectively of the used 0.25 micrometre P(A-I)/GR counterface, showing severe polishing and a thinner, less lumpy transferred film. Sliding is from top to bottom in both cases.

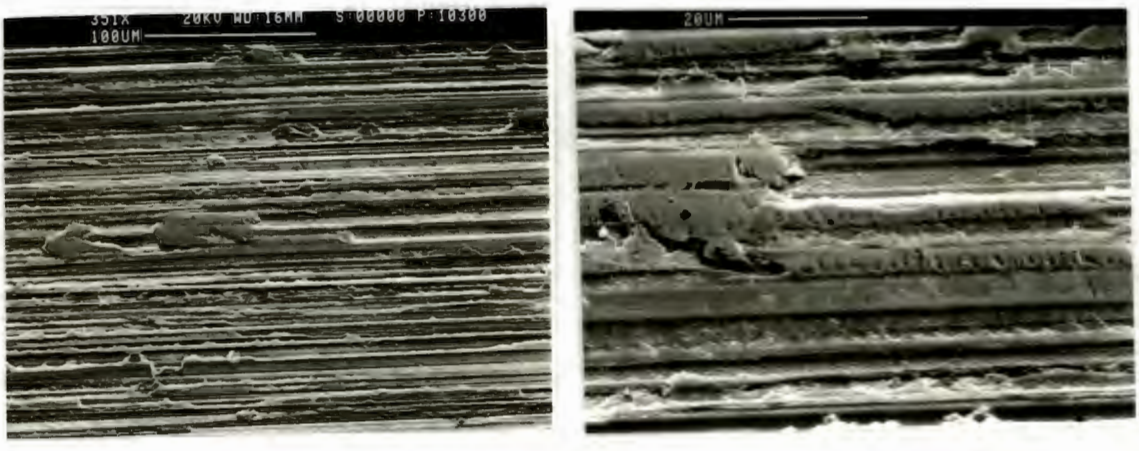

FIGURE 4.15(a) & (b) : Low and high magnifications respectively of the used 0.6 micrometre P(A-I)/GR counterface, showing slight polishing and a fairly lumpy transferred layer. Sliding is from bottom to top in both cases.

The polishing effect seen at the lower roughness has been mentioned elsewhere. Briscoe et al state that when carbon is used as a filler, only those carbons which abrade the counterface produce viable composites. They argue that the abrasion process may clean the counterface and ensure close contact between the metal or oxide and the polymer film [13] and that the optimum surface finish for film adhesion may be produced [12]. More recent work by Jain and Bahadur [37] on dry pin-on-disk tests of graphite filled poly(amide-imide) copolymer has shown a similar dependence of wear rate on counterface roughness to that found by the author. No mention of a polishing effect has been made however and yet their results show a virtual independence of wear rate on roughness below 0.43 micrometres R_a suggesting some sort of polishing effect. No micrographs are presented for this region of the curve shown in ref. [37] fig. 7 but it is possible that polishing of the AISI 1045 steel counterface did not occur because of its hardness of 55 HR_C (compared to the author's AISI 431 at 46-48 HR_C).

The virtual independence of the wear rate of P(A-I)/GR on counterface roughness can therefore probably be attributed to the materials ability to polish the smoother counterfaces and transfer a thin coherent film and to transfer a thicker film on rougher counterfaces, masking the effect of counterface asperities.

4.2.3.3 POM

POM shows higher wear rates than the other materials over the entire range of roughness but especially at the higher values of R_a. It is believed that this is related to the materials inability to form an appreciable transfer film even on smoother surfaces, with only a few small to medium (20-50 micrometres in size) transfer particles sparsely scattered over the counterface. An example of such a particle is shown in fig. 4.16.

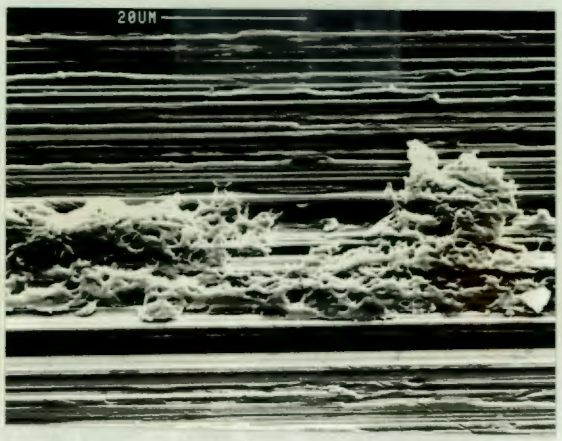

FIGURE 4.16 : Transferred POM particle on a 0.25 micrometre counterface. Sliding is from bottom to top.

The porous structure of the polymer (fig. 4.17) probably results in easier tearing of the material by the large asperities of the rougher counterfaces, resulting in high rates of wear.

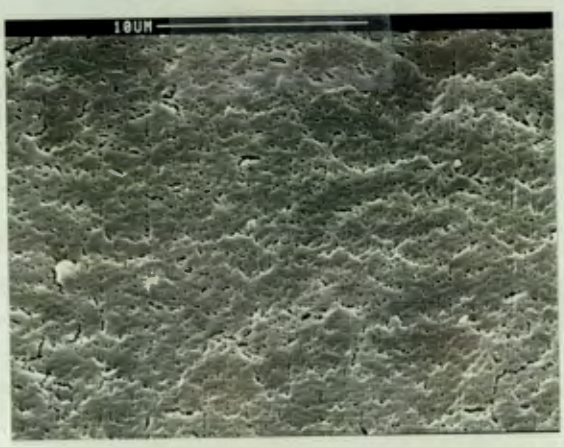

FIGURE 4.17 : POM surface from a 1 micrometre wear test showing the microporosity of this material. Note that void coalescence into microcracks has occurred.

In summary then, it appears that at 0.13 m/s and 5 MPa, all the materials will show an increase in wear rate as the counterface roughness is increased from 0.25 to 1 micrometre R_a. This is true also for all the other permutations of speed and pressure investigated, as can be seen in the summarised table of results in Appendix C.

4.3 THE EFFECT OF SLIDING VELOCITY

The effect of sliding velocity as a system parameter is particularly important because of the viscoelastic response to stress of a polymer and because of the generation of frictional heat. The dependence of wear rate of a polymeric material on the sliding velocity will therefore be related to the polymer's response to viscoelastic and thermal effects. Consideration of the wear data from the sliding velocity tests conducted in the present studies, shows two general types of response, which for brevity will be called Type I and Type II responses to increases in sliding velocity.

4.3.1 Type I Response

All of the materials, under most of the conditions of sliding, show a similar response to increases in the sliding velocity. Fig. 4.18(a) shows the wear rate versus sliding velocity plots for POM at pressures of 1 and 5 MPa and fig 4.18(b) shows an expansion of the plot for the 1 MPa case.

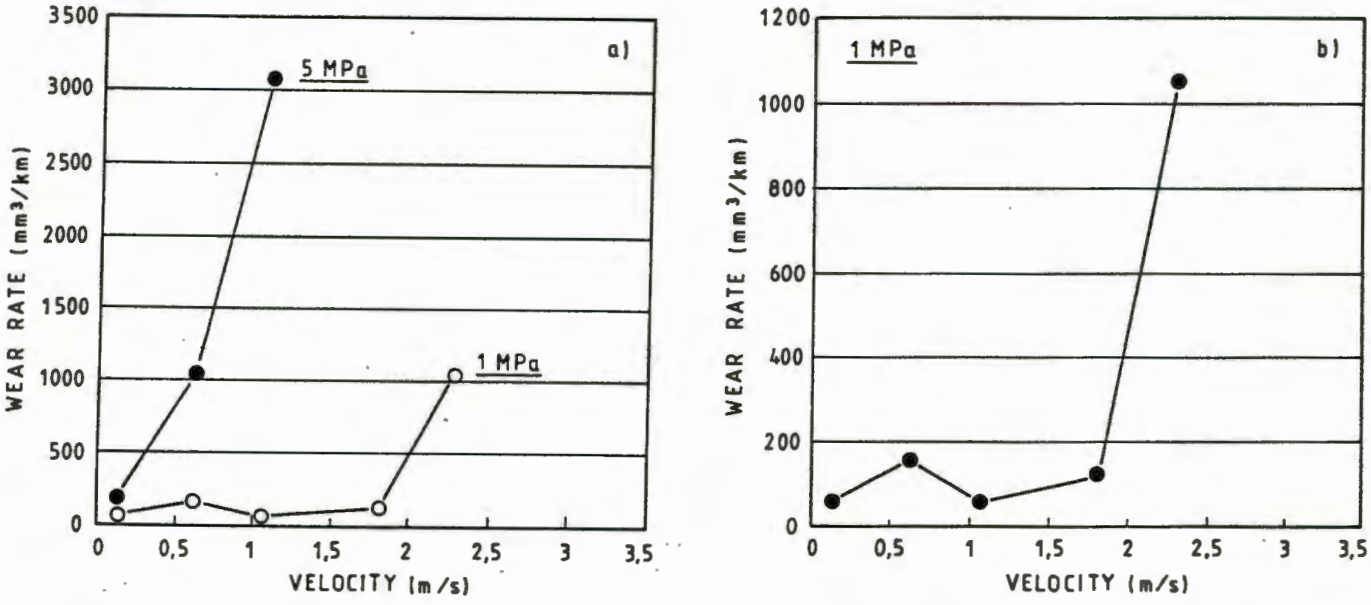

FIGURE 4.18(a) & (b) : Wear rate vs sliding velocity results for POM showing (a): responses at both testing pressures, and (b): an expanded scale for the response at the lower pressure. The counter-face roughness used was 1 micrometre.

The general trends which are shown by POM are fairly typical of all the other materials as well, but not necessarily under identical conditions of applied load and counterface roughness. UHMWPE for instance shows at 5 MPa, a similar trend to that shown by POM at 1 MPa. PETP behaves in a similar way at 1 MPa but with the positions of maxima in the curve shifted to slightly higher velocities. This can be seen in fig. 4.19(a) and (b).

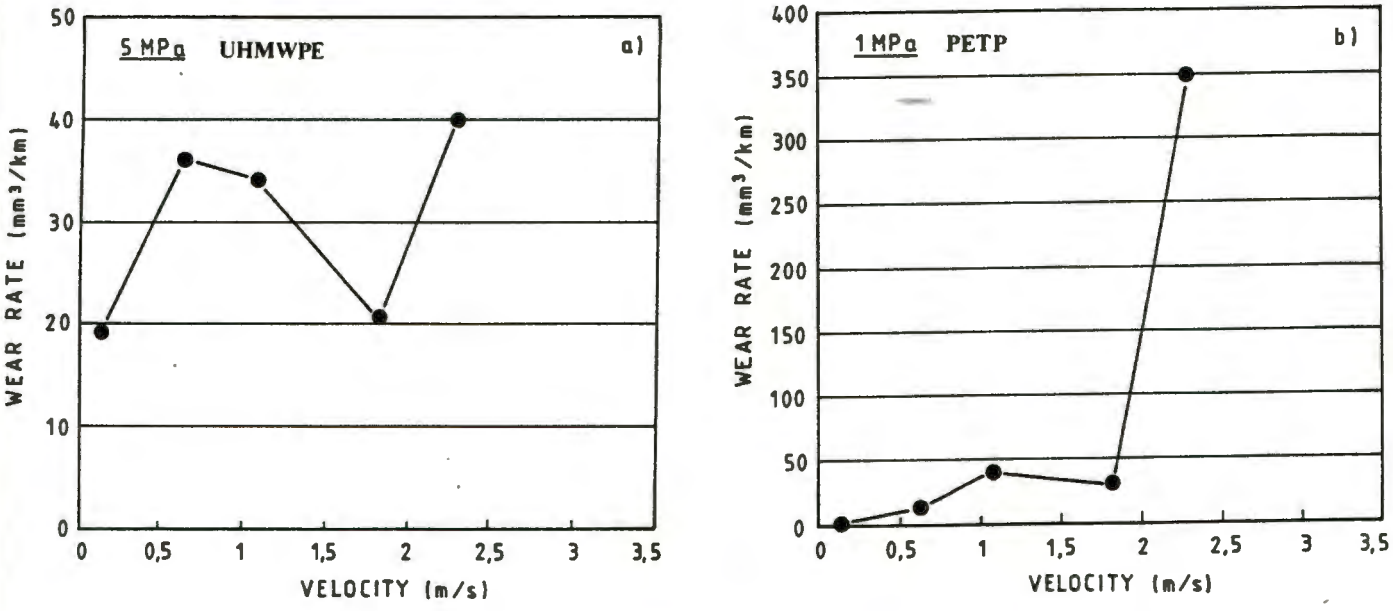

FIGURE 4.19(a) & (b) : The behaviour of UHMWPE at 5 MPa and of PETP at 1 MPa respectively. Compare with fig. 4.18(b). The counterface roughness used was 1 micrometre.

It is possible to formulate a model for this behaviour (Type I) and this model is proposed in fig. 4.20 overleaf.

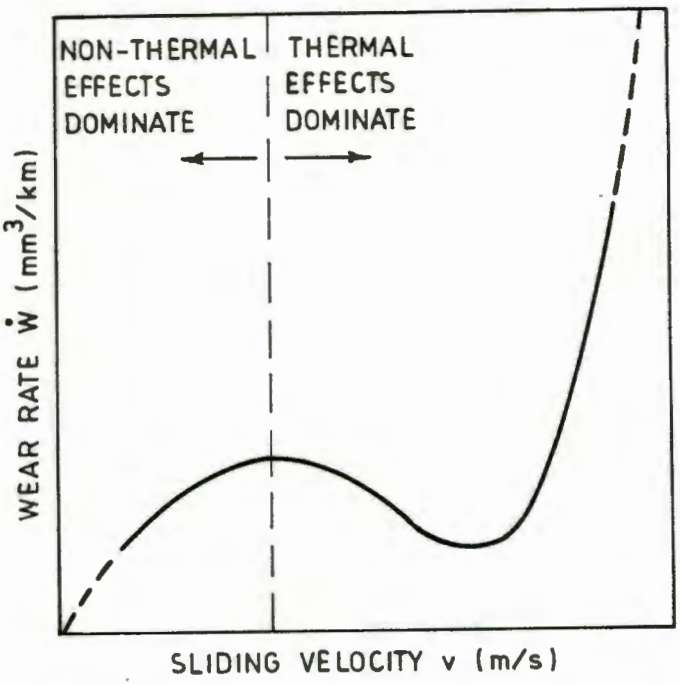

FIGURE 4.20 : Proposed model for the Type I behaviour of a polymeric material's wear rate in response to changes in the sliding velocity.

This model predicts an initial increase in the wear rate, as velocity is increased, until a local maximum is reached, whereafter the wear rate drops down to a local minimum and finally, shows a rapid rise as velocity is increased further. This type of behaviour has been found in other wear tests [32,1] and the following suggestions have been made to attempt to explain the observed trends. Evans and Lacaster [32] state that the maxima occurring at relatively low speeds are qualitatively consistent with viscoelastic (rate of strain) effects, and the subsequent minima and rapid increases in wear result from temperature increases associated with high speeds. Anderson [1] shows plots of the specific wear rate of UHMWPE versus sliding speed for three different lubrication conditions which appear in fig. 4.21 overleaf. The temperatures shown are the sum of the measured pin and calculated flash temperature.

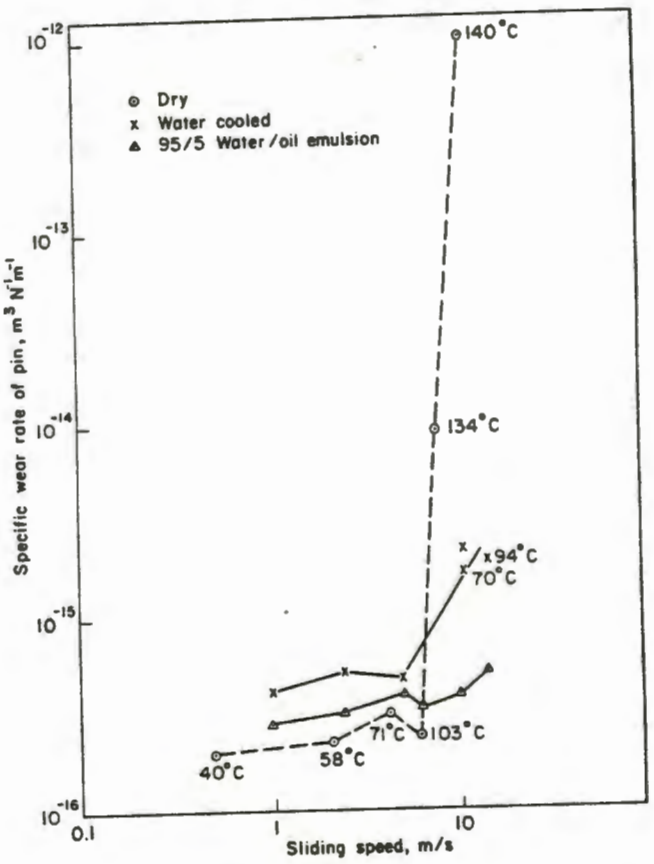

FIGURE 4.21 : The variation of specific wear rate of an UHMWPE pin on a steel disc with sliding speed (after [1]).

The results seem to follow the pattern of the model proposed by the author, with the positions of maxima and minima slightly shifted by lubrication conditions. The reasons for the shape of the curve in fig. 4.20 are not clear, but some suggestions are as follows. The rise in wear rate to the initial maximum is due to an increasingly brittle response of the polymer surface layers to the increasing rates of deformation (sliding speed) by counterface asperities. The increasingly brittle response of the polymer surface would result in the removal of brittle lumps or chips of material. This trend does not continue unabated however because of the thermal effects which begin to compete with the strain rate effects. The increase in temperature of the polymer surface due to the increase in sliding speed results in a decreasing brittleness allowing rearrangement rather than removal of the surface which tends to lower wear rates down to a local minimum. Competition between the strain rate and thermal effects thus gives the viscoelastic material an initially

increasing wear rate in which the former effect predominates, followed by a decreasing wear rate in which the latter effect is dominant. The rapid rise in the wear rate versus velocity curve as velocity is increased still further is due to gross thermal breakdown of the structure and mechanical properties of the polymer surface i.e. severe thermal softening and possibly melting. A POM surface from a 1 MPa, 2.268 m/s tests (the highest value in fig. 4.18(b)), is shown in fig. 4.22.

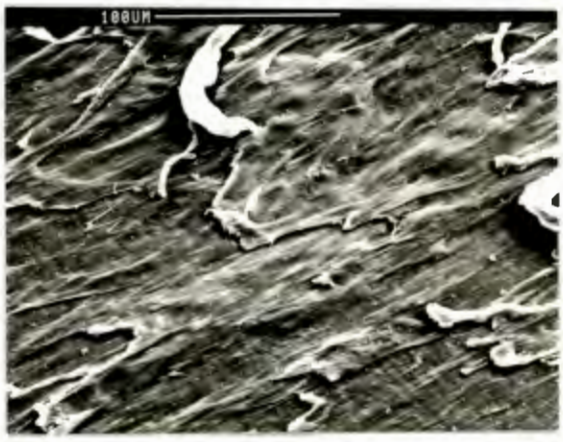

FIGURE 4.22 : POM surface. p = 1 MPa, v = 2.268 m/s, sliding direction is from top right to bottom left.

The surface of the POM appears to have been smeared while molten or semi-molten, with slivers of polymer or "stringers" having been extruded by counterface asperities.

Lhymn and Light [44], working with glass-fibre and carbon-fibre reinforced PBTP have found two regions in wear rate versus sliding velocity data. In the low velocity region, the specific wear rate tends to decrease as the sliding velocity increases, while in the high velocity region, the wear rate tends to increase with rising velocity. This type of behaviour has been found here for both the graphite filled poly(amide-imide) and the molybdenum disulphide filled polyamide (see fig. 4.23(a) and (b) respectively).

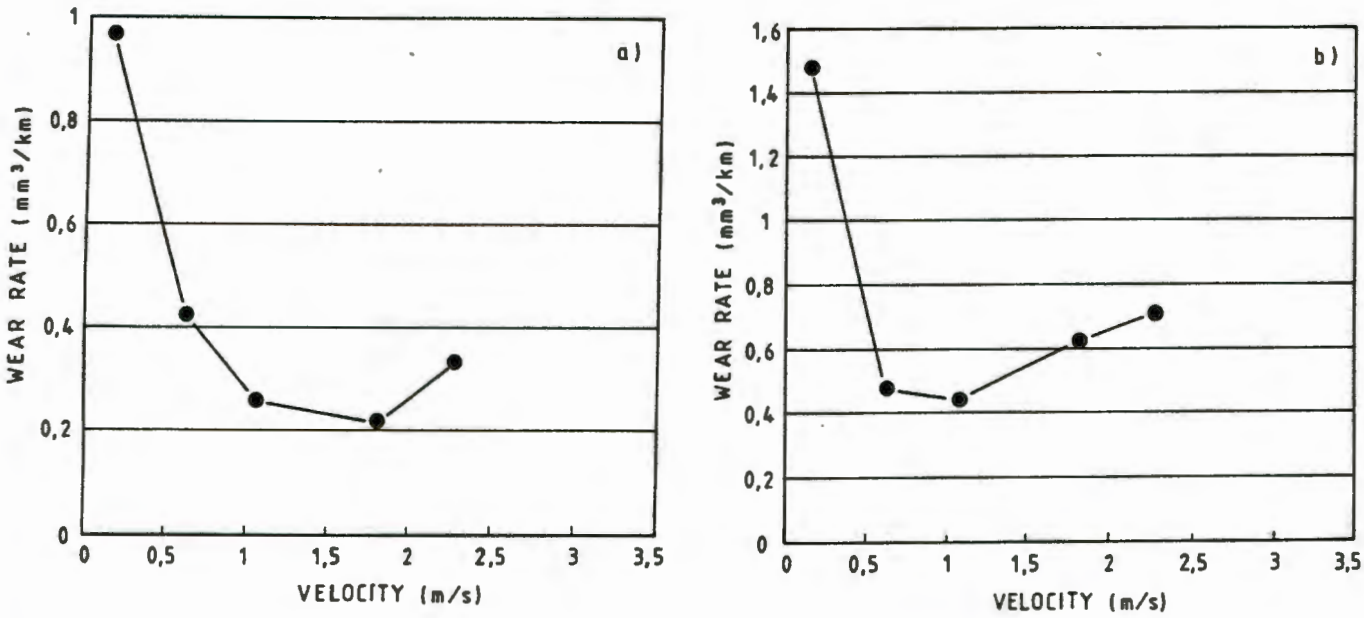

FIGURE 4.23 (a) and (b) : Wear rate vs velocity data for P(A-I)/GR and PA6/MoS_2 respectively. Counterface R_a = 0.25 micrometres and p = 1 MPa.

The explanation for such behaviour has been suggested [44] as being dependent on the physics of crack propagation and a consideration of the concept of thermal activation. An equation for the dependence of wear rate on sliding velocity in fibrous composites appears as :

$$W_s = A(1/V_s) \exp(-C/T)$$

where W_s is the specific wear rate, A is a constant, V_s is the sliding velocity, C is a constant and T is the local temperature at the sliding contact. T is assumed to vary with the sliding velocity either linearly or parabolically such that $T = k(V_s)^m$ where m = 1 or 2 and k is a constant. This gives :

$$W_s = A_1(1/V_s) \exp(-C_1/(V_s)^m) \quad \text{for high speeds}$$

and $$W_s = A_2(1/V_s) \quad \text{for low speeds}$$

At low sliding velocities, when the temperature rise at the contact spot is not significantly high, such that the frictional stress is not thermally activated, then the specific wear rate is inversely proportional to the sliding velocity.

When the temperature rise becomes significant, so that the deformation/frictional wear process can be thermally activated, then the latter exponential term dominates the wear rate. When V_s becomes very high then the wear rate increases as sliding velocity increases and the exponential term outweighs the linear term.

This argument for the explanation of the shape of the wear rate versus velocity curve was derived for fibrous composites, and its applicability to unfilled homopolymers is uncertain. It is possible that the behaviour shown by P(A-I)/GR and PA6/MoS_2 in fig. 4.23(a) and (b) respectively, conforms to such an explanation. It is also possible that the curves for these two cases are merely sections or regions within the model curve proposed and explained by the author. Whatever the correct explanation might be it is clear that the higher velocity region of the curve is dominated by thermal effects while the lower velocity region is dominated by non-thermal effects. Reference to Appendix C will show that, with few exceptions (Type II behaviour), the data follow the general trends seen in the model for Type I behaviour, or at least fit into a regime within the model curve.

4.3.1.1 Deviations from trends

It was noted that both POM and PETP under 1 MPa, 0.25 micron counterface conditions, showed a drop in the steady state wear rate when velocity was increased from 1.815 m/s to 2.268 m/s (Appendix C), which is contrary to the trends discussed above. It is believed that this is related to inconsistent but severe vibrations of the specimen and the experimental rig during high speed tests with the harder, more brittle materials like the two mentioned here. It was observed that consistent severe vibration produced weight losses up to ten times greater than when vibration was totally absent, for the same experimental parameters. This means that for a test involving say, six successive weight loss measurements, each of the weight losses recorded can be between unity and ten times that of the smallest value.

This gives a rather poor straight line fit to the data, and causes large (50 %) scatter between wear rate values for repeat tests. The reason for the existence of these vibrations is believed to be related to the geometry of the specimens and the configuration of the testing system. Small imperfections in the geometry of the system undoubtedly exist and some possible suggestions are laid out below.

a) The longitudinal axis of the drill shaft is not perpendicular to the turntable surface (fig. 3.6).

b) The longitudinal axis of the drill bit is not parallel to the drill shaft due to imperfections in the drill chuck (fig. 3.1).

c) The sliding face of the drill bit is not perpendicular to the longitudinal axis of the bit (Appendix B).

d) The upper and lower faces of the polymer disc are not parallel (Appendix B).

e) The stainless steel specimen seating block (fig. 3.2) does not have the bottom surface (which is in contact with the turntable discs) parallel to the upper surface on which the polymer specimen rests.

f) The sides of the stainless steel specimen seating block (which are in contact with the faces of the large external clamp) are not at 90° to the upper and lower surfaces of the block.

The existence of any or all of these faults in the testing system would result in imperfect alignment and mating of the wear surfaces of the counterface and the specimen. This leads to a slightly uneven distribution of the applied load over the wear surface of the polymer disc and the resulting instantaneous frictional drag forces will be slightly different in magnitude at two points diametrically

opposite one another on the disc surface. This causes a net displacement of the entire turntable assembly in the direction of the larger component of the "couple". At some instant later, the point of greater contact pressure (or "high spot") will have rotated through some angle ϕ so that the resultant of the uneven frictional couple will be pointing in a direction that is at an angle of ϕ to what it was the instant before. A net displacement of the turntable assembly in a direction at ϕ to that which occurred the instant before, will result. A continuation of the process through 360° of rotation will result in a precession of the turntable assembly axis about some central point, which at high frequency (high angular velocities) could be called vibration. The situation is further complicated by the assembly's attempt to recover from the original elastic deflection once the resultant of the couple moves to act along a different direction. This continual attempt at elastic recovery after each successive displacement is superimposed on the vibration pattern already established by the initial reactions to the uneven frictional couple.

Evidence to support this theory of uneven pressure distribution is to be found in examination of the counterface from a test in which vibration occurred. Opposing quadrants often show uneven amounts of transferred polymer, suggesting that the contact pressure on the two quadrants was uneven, with the heavier transfer occurring at the higher pressure quadrant.

Such vibrations will of course only be significant if frictional forces are likely to be significant, as is the case with high pressures and high velocities (due to the high rates of surface deformation required under these conditions if normal solid to solid contact is to be maintained). If such high rates of deformation are no longer necessary, either because velocity and pressure are decreased (under boundary lubrication conditions) or because complete solid to solid contact is not maintained

(due to the transition to partial EHL - see Section 2.4.4) then vibrations will cease to be significant and the wear rate will drop accordingly. In the case of POM and PETP, which was mentioned at the beginning of this subsection, it was noted that severe vibration disappeared and wear rates dropped (see fig. 4.24 below) when the velocity was increased from the second-highest to the highest value used under the lowest pressure used (1 MPa) and with the lowest counterface roughness used (0.25 micrometres R_a).

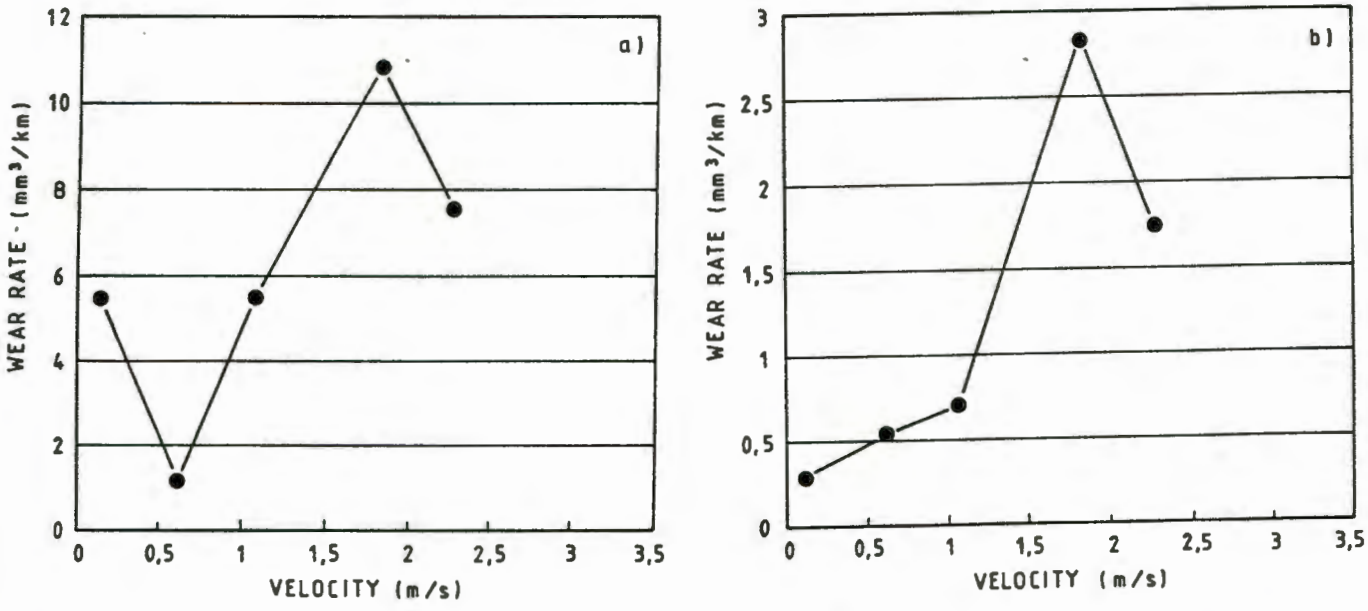

FIGURE 4.24(a) and (b) : Wear rate vs velocity for POM and PETP respectively. p = 1 MPa, R_a = 0.25 micrometres. (Compare with the model in fig. 4.20).

It is possible that the drop in wear rate as v is increased at low p and low R_a could be related to a transition to mixed lubrication, which is discussed below as a Type II response of wear rate to sliding velocity.

4.3.2 Type II Response

In cases where applied loads were light and sliding velocities high, it was found that some materials behave in a different way to the Type I trends discussed above. Fig. 4.25 shows the wear rate versus sliding velocity data for such a case.

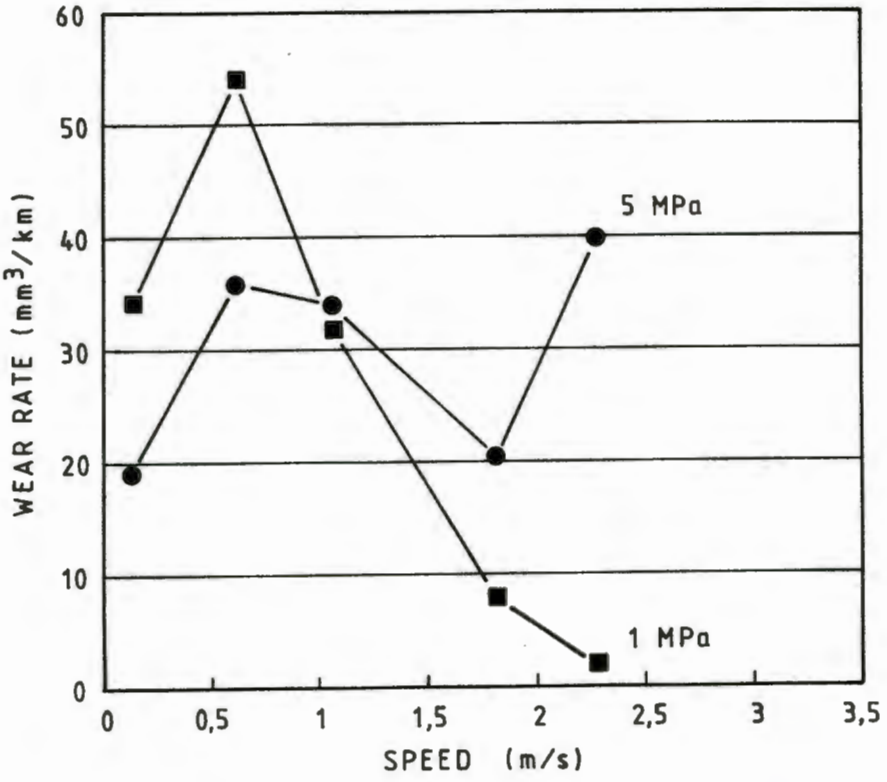

FIGURE 4.25 : Wear rate vs sliding velocity for UHMWPE.
R_a = 1 micrometre

The wear rate appears to follow a Type I trend at high normal load, but at low normal load it appears that increasing the velocity beyond a certain point causes a rapid decrease in the wear rate. This behaviour was observed in the case of UHMWPE/FILL as well, when sliding under the same conditions. At a lower value of counterface roughness a similar pattern was found. This behaviour was not seen under any conditions for any of the materials other than UHMWPE and UHMWPE/FILL except for the two cases mentioned at the end of the previous subsection. Reference to the section on lubrication in Chapter 2 will show that for a given applied load, increases in the velocity can result in load support from EHL either on an asperity scale or via geometric wedge formation. The partial separation of the surfaces by a wedge of lubricant is likely to result from elastic deflections of the polymer or its support system [25], and lower modulus materials will undergo this effect more easily (at lower velocities and higher loads) than higher modulus materials. Reference to Table 3.5 shows that UHMWPE and UHMWPE/FILL have much lower elastic moduli than those of the other materials and that they will therefore undergo at least partial EHL at lower velocities

or higher pressures than the stiffer materials. This reasoning is used to develop a model for Type II wear behaviour in fig. 4.26 below.

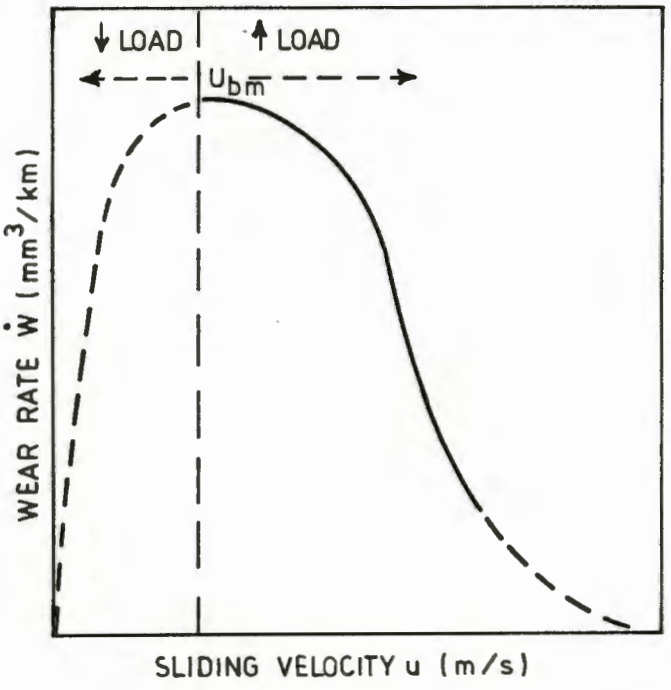

FIGURE 4.26 : Proposed model for Type II wear behaviour.

This model suggests that given a high enough sliding velocity, any relatively low modulus material should eventually display Type II behaviour provided that the lubricant properties such as viscosity remain unchanged. Thus, a stiffer material like PETP for instance, may follow the complete Type I trend until a sufficiently high sliding velocity allows a transition to mixed lubrication and a resulting drop in friction (vibration) and wear rate. This velocity may be lowered if the applied load is lowered or if conditions for wedge formation are improved. In this case, it is suggested that the onset of partial EHL by geometric wedge formation is assisted by the rounded off leading edges of the waterways on the counterface (see the description of specimen geometry in Chapter 3). SEM examination of the wear surfaces from the tests in fig. 4.25 shows that as velocity is increased, the large sheets of transfer on the counterface disappear and the polymer surface seems less deeply scored or less severely rucked up. This can be seen in fig. 4.27,

which is the highest velocity UHMWPE test surface from fig. 4.25.

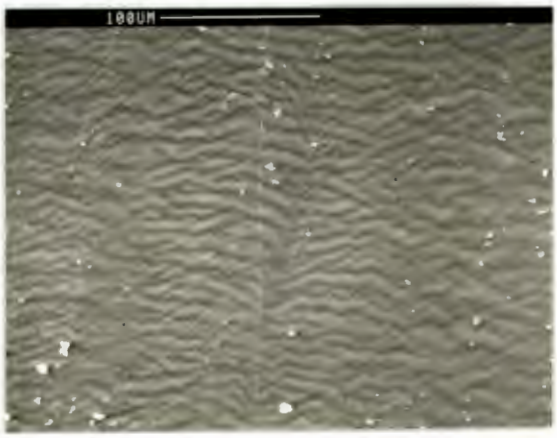

FIGURE 4.27 : UHMWPE surface from a 2.268 m/s test under 1 MPa with a 1 micrometre R_a counterface. Sliding is from bottom to top. Compare with fig. 4.6(b) which is a low velocity test.

4.4 THE EFFECT OF LOAD/PRESSURE

In order to study the effects of pressure on the wear behaviour of the six polymers of interest, the load applied during testing was varied at all the combinations of counterface roughness and velocity. The results of all these tests are shown in Appendix C, and for the purposes of discussion, some typical examples will be presented here in graphical form.

4.4.1 General Trends

The wear rate versus applied nominal pressure results, for a 1 micrometre counterface at a sliding velocity of 0.13 m/s, are summarised in figs. 4.30(a) and (b).

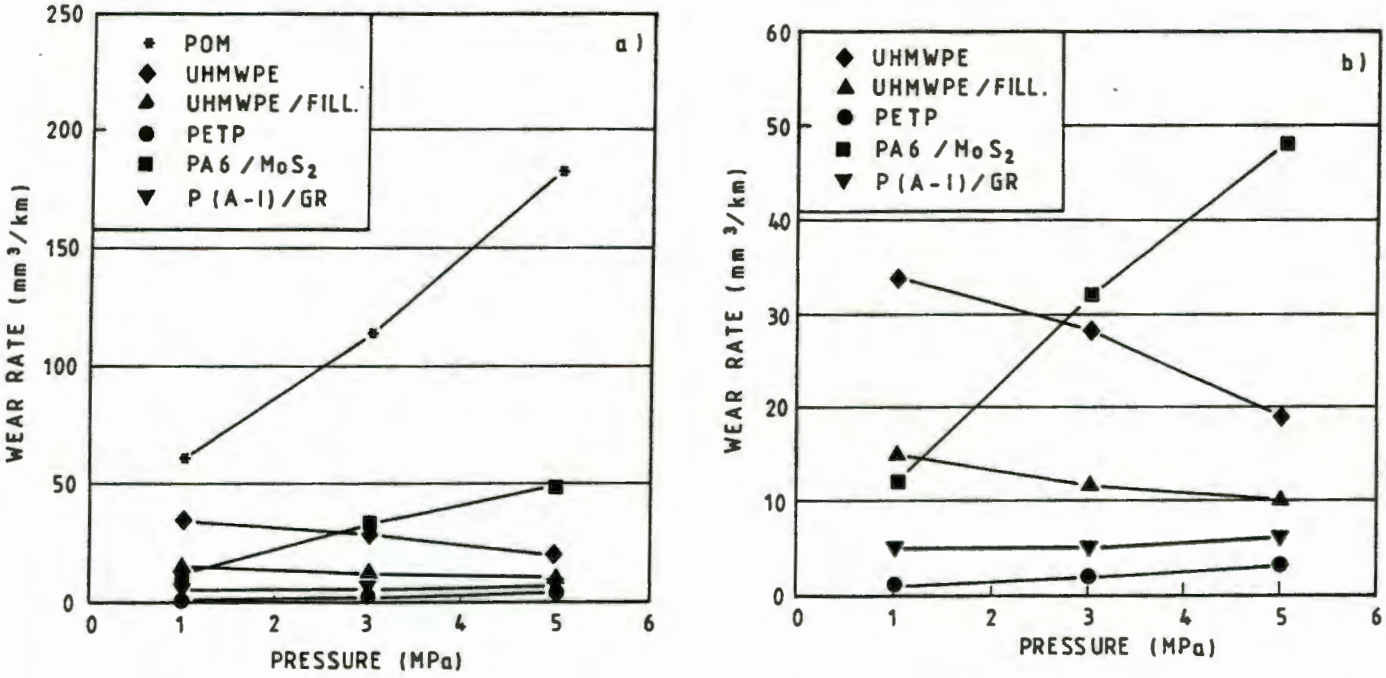

FIGURE 4.30(a) & (b) : The effect of pressure on wear rate for : (a) all the materials and (b) all the materials except POM. R_a = 1 micrometre, v = 0.13 m/s.

It is clear that for all the materials except UHMWPE and UHMWPE/FILL, there is a linear or nearly linear increase in the wear rate as the load is increased from 1 MPa through to 5 MPa. This trend will be discussed first.

4.4.2 Load vs Wear Rate Models

The simple models of wear developed in Sections 2.2.1 and 2.2.2 show that if frictional heating and softening can be neglected, the dependence of wear rate on applied load is linear for pure abrasion and a power function for pure fatigue wear, while adhesive wear theory predicts a direct proportionality. Evans and Lancaster [32] have shown results (see fig. 2.7) that indicate a direct proportionality up to a critical value of load. Similar results have been found by Anderson [2] for polyacetal and UHMWPE on mild steel, and by Jain and Bahadur [37] for graphite filled poly(amide-imide) on steel.

In the case of pure abrasion, an increase in the normal load would tend to push the sliding asperities of the counterface further into the polymer, allowing each cutting or gouging asperity to take a larger "bite". This would obviously result in an increase in wear. In the case of pure adhesion, an increase in the normal load would tend to force the smooth counterface and the polymer closer together, increasing the real area of contact A_r and the adhesive junction between metal and polymer. The increased adhesive forces would result in larger volumes of polymer being displaced and higher wear rates. For a fatigue wear situation counterface asperities produce successive deformation of the polymer surface until a wear particle becomes detached. An increase in the normal load would result in larger individual deformations at asperity tips for each pass of an asperity. The number of passes required to achieve sufficient deformation for detachment of a polymer wear particle from the polymer surface will be diminished and there will therefore be an increased rate of wear if load is increased.

Two of the six materials, namely PETP and P(A-I)/GR show only slight increases in steady state wear rate with load, and bearing in mind that scatter in these results can be up to fifteen percent, it is possible that their wear rates are virtually independent of load over this load range. The hardness values of these two materials are considerably greater than those of the other materials (Table 3.5), and in the predominantly abrasive/fatigue mechanism proposed in Section 4.1 for these materials under these conditions, this would have an effect. In either an abrasive or fatigue wear situation, the harder the material, the less responsive it will be to indentation and deformation by counterface asperities. An increase in load will cause a less significant increase in asperity-polymer interaction than for softer materials, and hence a less significant response of wear rate to increasing load. In the case of P(A-I)/GR, this effect is even more pronounced than with PETP (fig. 4.30) because of the increased hardness and load support by graphite particles. Jain and Bahadur [37] have found virtual load independence of wear rate for this material in the load range used by the author (see fig. 2.9). Furthermore, they state that the

lower wear rate for the graphite filled poly(amide-imide) copolymer relative to that for the unfilled material can be attributed to the load sharing by the graphite particles, an increase in thermal conductivity and the lubrication provided by the carbon-PTFE film.

4.4.3 Exceptions

Fig. 4.30(b) shows that there are two clear exceptions to the general trends and models discussed thus far. The materials UHMWPE and UHMWPE/FILL appear to have a decreasing wear rate versus load relationship through the load range used in these tests. Watanabe and Yamaguchi [63] have found similar behaviour for Nylon 6 within a certain load range, and this has been attributed to the influence of the interfacial temperature on the position of the shear plane. Increasing load results in increasing interfacial temperatures. The shear strength of the polymer/metal interface falls linearly as the temperature is increased, while that of the polymer itself follows a curved rather than a linear drop. Significant decreases in the polymer shear strength only occur at slightly higher temperatures than for the shear strength of the polymer metal interface (see fig. 2.8).

The net result is that within some temperature (load) range sliding will occur at the polymer metal interface rather than at some plane within the polymer itself resulting in a decrease in wear loss.

Lhymn [43] has found a decreasing specific wear rate versus load relationship for nylon-glass fibre composites on abrasive surfaces and for acetal/glass-fibre on steel plate. This behaviour is attributed to the lubricating effect of a softened polymer film at the contact spots.

Reference to Appendix C will show that at a counterface roughness of 0.25 micrometres all polymers show a slight increase in wear rate with applied pressure. There are therefore no exceptions to the model in this case. It is not clear why two of the materials should have different responses to nominal pressure at two different counterface roughnesses, but it is possible that this is related to the rates of surface deformation in each case. The low melting point of UHMWPE and UHMWPE/FILL could make them more susceptible to temperature effects at asperity contacts and it is possible that the higher rates of surface deformation, induced by the larger asperities found on a rougher counterface, are sufficient to cause the formation of a softened polymer film of the type suggested by Lhymn [43]. It is also possible that the subsurface layers of the polymer may become tougher, or less brittle, in response to the increased interfacial temperature produced by a rougher counterface than for a smoother counterface under the same load. This increased plasticity could result in gross rearrangement of the polymer surface by the counterface without actual formation of wear chips or debris, thus lowering actual volume losses from the polymer surface.

Figs. 4.31(a) and (b) are micrographs of a worn UHMWPE surface from 1 MPa and 5 MPa tests respectively.

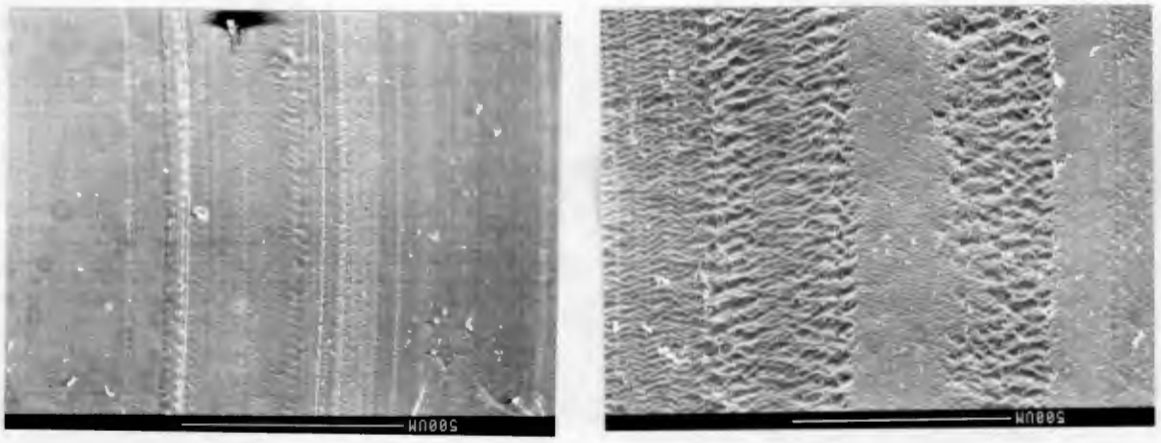

FIGURE 4.31(a) & (b) : Worn UHMWPE surfaces from 1 MPa and 5 MPa tests respectively. Counterface R_a = 1 micrometre, v = 0.13 m/s. Sliding direction is from bottom to top in both cases.

In both figs. 4.31(a) and (b) there are bands of wavy striations, the striations lying transverse to the direction of sliding. On the 5 MPa surface, the bands are broader and the striations more pronounced, while on the 1 MPa surface the bands are fewer in number and narrower. Similar behaviour is exhibited when considering 1 MPa and 5 MPa UHMWPE surfaces from 0.25 micrometre, 0.13 m/s tests. Any striations on the surfaces from the tests with the lower counterface roughness are uniformly less pronounced than those occurring on surfaces from the rougher counterface tests, but the relative differences in appearance beween the 1 MPa and 5 MPa cases seem to follow the same pattern as for the 1 micrometre conditions. Even though different modes of transfer appear to be present on the counterfaces of different roughness (see section 4.1), both 0.25 micrometre and 1 micrometre counterfaces show slightly heavier transfer in 5 MPa tests than in 1 MPa tests. The UHMWPE/FILL surfaces and counterfaces are similar in appearance to those of UHMWPE shown here. The observations made on wear surfaces from tests done at different pressures appear to show an increase in the severity of action of counterface asperities if the applied load is increased. However, these observations seem to be rather inconclusive in explaining the different responses of UHMWPE and UHMWPE/FILL to pressure increases when sliding against counterfaces of different roughness.

Evidence in support of or against the theories of Watanabe or Lhymn does not appear to be forthcoming, and it is clear that more work needs to be done on the effect of applied load, in order to clarify the reasons for the responses in wear rates.

CHAPTER 5

CONCLUSIONS

Examination of Chapter 3 shows that a laboratory test rig was developed which allowed unidirectional sliding wear tests to be performed over a wide range of experimental conditions in the presence of tapwater as a lubricant. These conditions encompassed those expected to be found in service (see Section 3.2) and it is believed that a reasonable simulation of the sliding conditions at the rotating tool holder on the hydraulic rockdrill, was achieved.

The conclusions reached in this study are that the wear of the polymeric materials tested is a function of (a) counterface roughness, (b) sliding velocity, (c) load and (d) type of material. The general trends found were as follows :

a) Increasing the counterface roughness from 0.25 micrometres through to 1 micrometre R_a had the effect of increasing the wear rates of the materials tested, in all cases. All the materials except UHMWPE/FILL showed rapid increases in the lower regions of roughness and less rapid increases in the higher regions of roughness. The graphite-filled poly(amide-imide) copolymer appeared to be the least sensitive to changes in counterface roughness. The trends and exceptions to trends observed are believed to be related to changes in the mechanism of material removal from the polymer surface and the explanations for these observations can be found in Section 4.2.

b) Increasing the sliding velocity from 0.13 $m.s^{-1}$ through to 2.27 $m.s^{-1}$ at different values of normal applied load resulted in two general types of trend in the wear rates of the materials tested.

i) The first (Type I) trend observed was an initial increase in wear rate, followed by a decrease and finally a rapid increase, as velocity was increased. This trend was followed by all the materials under most of the conditions of applied load and counterface roughness and explanations have been suggested in Section 4.3.1 in terms of the viscoelastic response of the materials to strain rate and temperature.

ii) The second (Type II) trend observed was a significant decrease in the wear rate and apparent surface damage of the low modulus materials (UHMWPE and UHMWPE/FILL) above a certain sliding velocity. This was explained in terms of the elastic moduli of the materials and their relationship to the velocity required for a transition from a state of boundary lubrication to that of partial elastohydrodynamic lubrication. The discussion of this trend appears in Section 4.3.2.

c) Increases in the applied load over a range of velocities and counterface roughnesses had the effect of increasing the wear rates of all the materials under some of the conditions. The two exceptions to this were UHMWPE and UHMWPE/FILL which appear to show a decreasing wear rate versus load relationship over this load range when a counterface roughness of 1 micrometre R_a is used. These trends have been discussed in Section 4.4 in terms of the material's response to increased interaction with counterface asperities and thermal effects from load variations.

d) The relative wear rates of the materials tested obviously differed from one test condition to another but some general conclusions about the wear resistance of individual materials can be made.

i) By far the best performer in the majority of cases was UHMWPE/FILL, which showed the lowest wear rates at low and medium counterface roughnesses and also at high counterface roughnesses if low pressures and high velocities were used. No severe chattering occurred with this material even at high velocities, high loads and high counterface roughnesses, nor did it display any significant water absorption or swelling. It appears that this material performs the best across a wide range of conditions. Even though it may have higher wear rates than for example the polyester, when slid against rough counterfaces, it does not respond catastrophically if velocity is severely increased

(in fact this material shows marked decreases in wear rate as velocity is increased if loads are sufficiently low) nor does it lose its superior wear resistance at high loads.

ii) POM showed consistently worse performance than the other polymers under all conditions.

iii) At low sliding velocities PETP was found to have an excellent wear resistance, which was found to be generally insensitive to changes in the counterface roughness.

iv) P(A-I)/GR showed a general insensitivity in wear rate to changes in counterface roughness. It was noted that if the initial value of counterface roughness is low enough (in the region of 0.2 to 0.3 micrometres R_a) considerable smoothing of the counterface asperities can be achieved by the polishing action of this hard polymer on the steel. Relative to the other materials, P(A-I)/GR did not perform quite as well at high velocities and loads under less severe conditions. Comparable in terms of wear resistance to UHMWPE or UHMWPE/FILL at low sliding velocities, the poly(amide-imide) suffered severe vibration and impact wear at high velocities, whereupon wear rates became catastrophic.

v) UHMWPE showed good wear resistance under all conditions and did not suffer severe vibration at high loads and velocities. At low loads this material showed significant decreases in wear rate above a certain sliding velocity.

vi) PA6/MoS_2 displayed moderate wear resistance under most conditions along with considerable water absorption and swelling.

CHAPTER 6

RECOMMENDATIONS

1) (a) The trends observed for the effects of counterface roughness pose an interesting question of practical significance : In an in-service situation where steel components rub against polymeric bearings or seals there are two possibilities when faced with the choice of specifying the surface finish of the steel component. Should the rougher (say 1 micrometre) or the smoother (say 0.2 micrometres) finish be specified? In the former case, wear rates of the polymeric components will be higher, but fluctuations in or deviations from a specified finish (either due to incorrect finishing procedures or damage of the surface by foreign bodies) will not have a severe effect on the expected wear rates and therefore the service life of components can be accurately estimated. In the latter case wear rates will be lower, provided that the surface finishes of steel components remain according to specification, since at low counterface roughnesses small changes in surface finish cause large changes in wear rate and therefore, an unpredictability in service life. In underground applications such as those of the South African mining industry, where entrainment of abrasive particles into hydraulic fluids is highly likely, it is recommended that the designer consider the question of specification of the surface finish of steel components.

(b) The response of wear rate to smoother counterfaces than those used in the present studies should be investigated in order to determine if relative ranking in terms of wear resistance remains constant for all counterface roughnesses.

(c) More fundamental or academic considerations should be directed toward achieving an understanding of how material properties and the environment influence the formation of polymer transfer films.

2) The stepwise rather than continuous variation of the sliding velocity by means of the repositioning of spur gears is seen as a limitation in the present studies. A more complete picture of the trends observed would be found with a system that allows a continuous variation in the setting of velocity values. Inherent imperfections in the design of the laboratory wear testing rig are believed to cause excessive vibration in some cases at high velocities. Therefore, it is recommended that future work be carried out on a system that allows continuous variation of sliding velocity and that has a relatively simple geometry. Such requirements would probably be satisfied by a pin-on-disc system with a thyristor speed controller on the motor.

3) The effect of normal applied load on the wear rate of polymeric materials needs further investigation in order to clarify the reasons for the trends observed.

4) The work covered in this study has been done under water lubricated conditions and it is recommended that this work be extended to dry sliding conditions. This will give an assessment of whether or not the materials which have shown superior wear resistance, such as UHMWPE/FILL, will continue to do so for the same experimental values of load, velocity and counterface roughness as in the lubricated condition. The molybdenum disulphide filled polyamide (which absorbed water and showed considerable swelling) should be included in the investigation of performances under dry conditions as it is believed that without swelling and plasticisation of surface layers by water absorption, this material will show a promising wear resistance.

REFERENCES

1. ANDERSON, J.C. : "High Density and Ultra High Molecular Weight Polyethylenes : Their Wear Properties and Bearing Applications", Trib. Int. (FEB 1982), 43-47.

2. ANDERSON, J.C. : "Wear of commercially available plastic materials", Trib. Int., 15, 1, 255-263.

3. ANDERSON, J.C., ROBBINS, E.J. : "The Role of Wear Debris in the Wear of Some Polymer Composites at High Loads", in Ludema K.C. (ed), Proc Conf. Wear of Materials (1981), ASME, 539-543.

4. ARCHARD, J.F., HIRST, W. (1956) : Proc. R. Soc. London Ser., A236, p397.

5. ARKLES, B.C., SHIRESON, M.J. : Wear, 39 (1976), 177.

6. ATKINS, A.G., OMAR, M.K. : "Load Dependence of Fatigue Wear in Polymers", in Ludema K.C. (ed), Proc. Conf. Wear of Materials (1987), ASME, 405-409.

7. BAHADUR, S., TABOR, D. : Wear, 98 (1984), 1.

8. BAHADUR, S., TABOR, D. : Polymer Wear and Its Control, ACS Symp. Series 287, Lee L.H. (ed) (1985), 253.

9. BARTENEV, G.M., LAVERENTEV, V.V. : "Friction and Wear of Polymers", in Tribology Series, 6, Elsevier, (1981).

10. BELY, V.A., SVIRIDENOK, A.I., PETROKOVETS, M.I., SAVKIN, V.G. : "Friction and Wear in Polymer Based Materials", Pergamon, (1982).

11. BRAINARD, W.A., BUCKLEY, D.H. : "Adhesion and Friction of PTFE in Contact With Metals as Studied by Auger Spectroscopy, Field Ion and Scanning Electron Microscopy", Wear, 26 (1973), 75-93.

12. BRISCOE, B. : "Wear of Polymers : An Essay on Fundamental Aspects", Trib. Int., 14, No. 4, (Aug 1981), 231-243.

13. BRISCOE, B.J., STEWARD , M.P., GROSZEK, A. : "The Effect of Carbon Aspect Ratio on the Friction and Wear of PTFE", Wear, 42 (1977), 99-108.

14. BRISCOE, B.J., Ni Z. : "Friction and Wear of Gamma Irradiated PTFE", Wear, 100 (1984), 221-242.

15. BRISCOE, B.J. : "Tribology of Polymers : State of an Art", in Mittal K.L. (ed), Physico-chem. Aspects of Polymer Surfaces, Plenum New York (1982), 387.

16. BROWN, K.J., ATKINSON, J.R., DOWSON, D., WRIGHT, V. : Wear, 40 (1976), 255.

17. BROWN, K.J. : "A Study of the Wear of Polyethylene", PhD thesis, Leeds University (1975), 97.

18. BUCKLEY, D.H. : "Introductory Remarks - Friction and Wear of Polymeric Composites", in Lee L.H. (ed), Advances in Polymer Friction and Wear, Plenum, New York, (1974), 601-603.

19. BURWELL, J.T. : Wear, 1 (1957), 119.

20. CUDWORTH, C.J., HIGGINSON, G.R. : "Friction of Lubricated Soft Surface Layers", Wear, 37 (1976), 299.

21. CZICHOS, H. : "Influence of Adhesive and Abrasive Mechanisms on The Tribological Behaviour of Thermoplastic Polymers", Wear, 88 (1983), 27-43.

22. CZICHOS, H. : "Tribology. A systems approach to the Science and Technology of Friction, Lubrication adn Wear", Elsevier, Amsterdam (1978).

23. DAVIES, C.B. : "A Review of Boundary Lubrication", Wear, 1, 245-253.

24. DEUTSCHMAN, A.D., MICHELS, W.J., WILSON, C.E. : "Machine Design : Theory and Practice", MacMillan, New York (1975).

25. DICKENS, P.M., SULLIVAN , J.L., LANCASTER, J.K. : "Speed Effects on The Dry and Lubricated Wear of Polymers", Wear, 112 (1986), 273-289.

26. DOBRY, A. : "The Transitions Between Boundary, Mixed and Hydrodynamic Lubrication", Wear, 1 (1964), 290-297.

27. DOWSON, D., CHALLEN, J.M., HOLMES, K. ATKINSON, J.R. : "The Influence of Counterface Roughness on The Wear Rate of Polyethylene", Proc. 7th Leeds-Lyon Symp. on Tribology (1976), I Mech E, 99-102.

28. DOWSON, D., EL-HADY DIAB, M., GILLIS, B.J., ATKINSON, J.R. : "Influence of Counterface Topography on the Wear of UHMWPE under Wet or Dry Conditions", in Lee L.H. (ed), Polymer Wear and Its Control, ACS (1985), 171-187.

29. EGORENKOV : Soviet Materials Science, 9 (1973), 279.

30. EISS, N.S. Jr, MILLOY, S.C. : "The Effect of Asperity Curvature on Polymer Wear", in Ludema K.C. (ed) Proc. Conf. Wear of Materials (1983), ASME, 650-656.

31. ENGEL, L., KLINGELE, H., EHRENSTEIN, G.W., SCHAPER, H. : "An Atlas of Polymer Damage", Wolfe, London, 1981.

32. EVANS, D.C., LANCASTER J.K. : "Wear of Polymers", in Treatise on Mat. Sci. and Technology, Academic Press Inc., 13, 86-134 (1979).

33. HALLIDAY, J.S. : Proc. Inst. Mech. Eng., 169 (1955), 777.

34. HERTZBERG, R.W. : "Deformation and Fracture Mechanics of Engineering Materials", 598-601, Wiley and Sons (1983).

35. HOLLANDER, A.E., LANCASTER, J.K. : Wear, 25 (1973), 155.

36. HOLMBERG, K., WICKSTROM, G. : "Friction and Wear Tests of Polymers", Wear, 115 (1987), 95-105.

37. JAIN, V.K., BAHADUR,S. :"Tribological Behaviour of Unfilled and Filled Poly (amide-imide) Copolymer", Ludema K.C. (ed), Proc. Conf. Wear of Materials (1987), ASME, 389-395.

38. KRAGHELSKII, I.V., NEPOMNYASCHII, E.F. : Wear, 8 (1965), 303.

39. LANCASTER, J.K.: Wear, 14 (1969), 223.

40. LANCASTER, J.K. : "Friction and Wear of Polymers", in Jenkins A.D. (ed), Polymer Science, North-Holland, Amsterdam (1972), ch14.

41. LANCASTER, J.K.: "The Lubricated Wear of Polymers", Proc. 11th Leeds-Lyon Symp. Lub. Wear (1985), Butterworths, London.

42. LLOYD, A.I.G. : "The Sliding Wear of UHMWPE Against Steel", MSc thesis, University of Cape Town (1986), 157.

43. LHYMN, C. : "Effect of Normal Load on Specific Wear Rate of Fibrous Composites", Wear, 120 (1987), 1-27.

44. LHYMN, C., LIGHT, R. : "Effect of Sliding Velocity on Wear Rate of Fibrous Polymer Composites", Wear, 116 (1987), 343-359.

45. MATSUBARA, K., WATANABE, M. : Wear, 10 (1967), 214.

46. McGHEE, A.C., DHARAN, C.K.H., FINNIE, I. : "Abrasive Wear of Graphite Fibre Reinforced Composite Materials", Wear, 114 (1987), 97-107.

47. MILLER, D. : "Rock Drilling with Impregnated Diamond Microbits", PhD thesis, University of Cape Town (1986).

48. MOORE, D.F. : "The Friction and Lubrication of Elastomers", Pergamon, Oxford (1972).

49. OECD (1969) : Friction, Wear and Lubrication - Terms and Definitions. Resident Group on Wear of Engineering Materials, Paris.

50. PLAY, D. : "Counterface Roughness Effect on the Dry Steady State Wear of Self Lubricating Polyimide Composites", Trans. ASME, J. Tribology, 106 (1984), 177-184.

51. RATNER, S.B., FARBERONA, I.I., RADYUKEVICH, O.V., LURE, E.G. : Sov. Plas., 7 (1964), 7.

52. ROWE, C.N. : "Lubricated Wear", Wear Control Handbook, ASME, New York, (1980), 143-160.

53. SHEN, C., DUMBLETON, J.H. : Wear, 30 (1974), 349.

54. STEWARD, M.P., : "Friction and Wear of PTFE Composites", PhD thesis, Cambridge University (1978).

55. SUH, N.P. : "Delamination Theory of Wear", Wear, 25 (1973), 111-124.

56. SWIKERT, M.A., JOHNSON, R.L. : "Simulated Studies of Wear and Friction in Total Hip Prosthesis Components with Various Ball Sizes and Surface Finishes", NASA technical note D-8174 (1976).

57. SVIRIDYONOK, A.I., NEVZOROV, V.V., PLESKACHEVSKII, Y.M. : "On the Role of Friction Transfer in the Wear of Some Thermoplastics", Ref 37, 439-443.

58. TANAKA, K., UCHIYAMA, Y. : "Friction, Wear and Surface Melting of Crystalline Polymers", in Lee L.H. (ed), Advances in Polymer Friction and Wear, Polymer Science and Technology, 5A and 5B (1974).

59. TANAKA, K. : "Friction and Wear of Glass and Carbon Filled Thermoplastic Polymers", in Ludema K.C. (ed), Proc. Conf. Wear of Materials, (1977), ASME 510-517.

60. TANAKA, K., NAGAI, T. : "Effect of Counterface Roughness on Friction and Wear of PTFE and PE", in Ludema K.C. (ed), Proc. Conf. Wear of Materials, (1985), ASME, 397-404.

61. TANAKA, K., YAMADA, Y. : "Effect of Counterface Roughness on Friction and Wear of PE under Sliding Conditions Involving Surface Melting", in Ludema K.C. (ed), Proc. Conf. Wear of Materials (1987), ASME, 407-414.

62. TANAKA, K., YAMADA, Y. : "Influence of Counterface Roughness on Friction and Wear of PTFE and POM Based Composites", Proc. Conf. Tribology - Friction, Lubrication and Wear, I Mech E (1987), 219-226.

63. WATANABE, M., YAMAGUCHI, H. : "The Friction and Wear Properties of Nylon", Wear, 110 (1986), 79-388.

64. WOLVERTON, M.P., THEBERGE, J.E. : "How Plastic Composites Wear Against Metals", Machine Design, (6/2/1986), 67-71.

65 WYATT, L.M. (ed) : "Thermoplastics", Fulmer Materials Optimizer, 3, 1.

APPENDIX A

Calculation of the average tangential velocity given the angular velocity in revolutions per minute and the specimen geometry.

From consideration of the counterface geometry (Appendix B) :

$$C_i=[2\pi r_i] - [(4x2\theta /360^\circ)x2\pi r_i]$$

where C_i = inner circumference
r_i = inner radius
2θ = angle subtended by the arc across the waterway (the arc is that part of the inner circumference which is "missing" due to the presence of the slot or waterway through the tube wall.)

This is illustrated in fig. A.1 below.

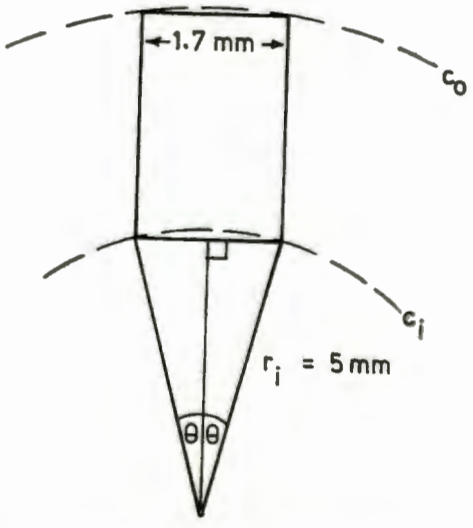

FIGURE A.1 : Calculation of the missing arc length. Drawing not to scale.

Thus, $C_i=[2\pi 5] - [(4x[2 \arcsin \frac{1.7/2}{5}]/360^\circ)x2\pi 5]$

$= 31.416 - 6.835$ mm

$= 24.58$ mm

Similarly/.....

Similarly, the outer circumference Co = 53.19 mm.
Thus the inner and outer distances which the polymeric disc surface "travels" (or sees the counterface travel past it) in one revolution, are known.
Average distance/rev = 38.885 mm
At 200 rpm, $v = (38.885 \text{ mm} \times 200 \text{ min}^{-1}/60\text{s.min}^{-1})/1000 \text{ mm. m}^{-1}$.

Therefore $v = 0.130$ m/s at 200 rpm

Similarly for the other values of angular velocity.

STEEL COUNTERFACE

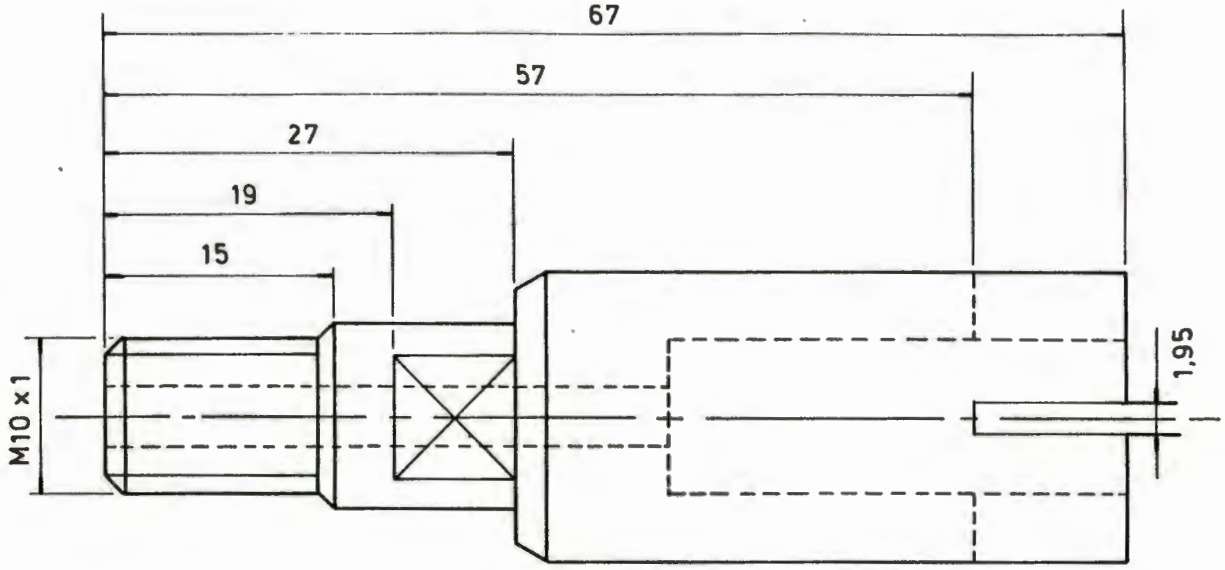

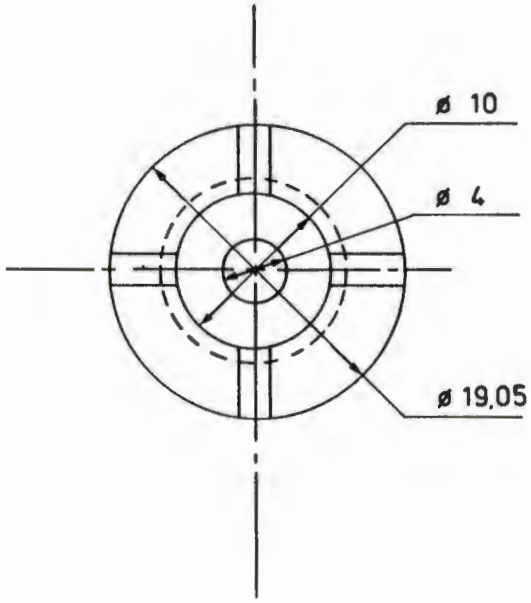

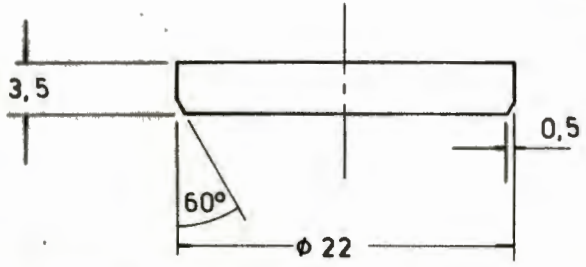

POLYMER DISC SPECIMEN

APPENDIX B

DEPARTMENT OF MATERIALS ENGINEERING			UNIVERSITY OF CAPE TOWN	
		DETAIL	WORK CATEGORY MSc THESIS	
		SCALE 2 : 1		
STUDENT C. CLARKE	DRAWN BY C. CLARKE		WORK SUPERVISED BY M. BATHO	
SUPERVISOR PROF. C. ALLEN				

APPENDIX C

Wear rates appear as mm^3/km for each condition of velocity, pressure and counterface roughness.

UHMWPE

		v(m.s^{-1}) 0.130	0.616	1.063	1.815	2.268		
P(MPa)	1	33.9	54.0	32.0	8.00	2.00	1	R_a(um)
	3	28.4	-	-	-	-	1	
	5	19.0	36.0	34.0	20.5	40.0	1	
	1	0	3.50	3.00	0.28	0.44	0.25	
	5	1.74	0.90	1.69	3.77	6.62	0.25	
	5	16.1	-	-	-	-	0.6	

UHMWPE/FILL

		v(m.s^{-1}) 0.130	0.616	1.063	1.815	2.268		
P(MPa)	1	15.0	4.00	3.00	2.00	1.00	1	R_a(um)
	3	11.6	-	-	-	-	1	
	5	10.0	5.00	10.0	15.0	30.0	1	
	1	0	0	0	0	0	0.25	
	5	0	0	0.065	0.084	0.15	0.25	
	5	1.34	-	-	-	-	0.6	

PA6/MoS_2

		v(m.s^{-1}) 0.130	0.616	1.063	1.815	2.268		
P(MPa)	1	12.0	18.1	16.0	24.1	16.0	1	R_a(um)
	3	32.1	-	-	-	-	1	
	5	48.0	119	67.0	98.2	88.0	1	
	1	1.48	0.477	0.440	0.623	0.709	0.25	
	5	1.93	9.83	21.0	7.16	69.5	0.25	
	5	43.3	-	-	-	-	0.60	

P(A-I)/GR

		v(m.s^{-1}) 0.130	0.616	1.063	1.815	2.268		
P(MPa)	1	5.00	3.00	4.00	4.00	3.00	1	R_a(um)
	3	5.02	-	-	-	-	1	
	5	6.00	17.0	86.0	-	-	1	
	1	0.969	0.425	0.257	0.215	0.331	0.25	
	5	2.67	1.89	1.64	9.49	24.3	0.25	
	5	5.56	-	-	-	-	0.60	

PETP

		v(m.s^{-1}) 0.130	0.616	1.063	1.815	2.268		
P(MPa)	1	1.00	12.0	40.0	29.9	350	1	R_a(um)
	3	1.87	-	-	-	-	1	
	5	3.00	2631	3070	-	-	1	
	1	0.294	0.538	0.704	2.85	1.75	0.25	
	5	1.14	37.0	163	1439	7210	0.25	
	5	2.81	-	-	-	-	0.60	

POM

		v(m.s^{-1}) 0.130	0.616	1.063	1.815	2.268		
P(MPa)	1	60.0	160	58.1	124	1050	1	R_a(um)
	3	113	-	-	-	-	1	
	5	182	1040	3070	-	-	1	
	1	5.48	1.16	5.45	10.9	7.57	0.25	
	5	14.0	30.4	1.16	156	1612	0.25	
	5	126	-	-	-	-	0.60	